Report Number COO-2232B-58

A PHENOMENOLOGICAL ANALYSIS OF TOTAL CROSS SECTION MEASUREMENTS AT N.A.L.

R.E. Hendrick, P. Langacker,(i) B.E. Lautrup,(ii) S.J. Orfanidis,(iii) and V. Rittenberg(iv)

The Rockefeller University, New York, New York 10021

---

*Work supported in part by the U.S. Atomic Energy Commission under Contract Number AT(11-1)-2232.

(i) Address after Sept. 1, 1974, The University of Pennsylvania, Philadelphia, PA 19104.

(ii) Address after Aug. 1, 1974, The Niels Bohr Institute, Copenhagen, Denmark.

(iii) Address after Sept. 1, 1974, New York University, New York, NY 10012.

(iv) On leave from the Tel-Aviv University, Tel-Aviv, Israel.

DISCLAIMER

Abstract

The available high energy total cross section data for $\pi^{\pm}$,$K^{\pm}$,p, and $\bar{p}$ scattering on protons and deuterons are analyzed. It is found that the diffractive (non-falling) components of the cross sections are compatible with several different functional forms for the energy dependence, including one in which σ_{K^+p},σ_{π^+p}, and σ_{pp} will rise asymptotically as ln s with coefficients in the ratios predicted by SU(3) and the naive quark model. The falling components of the cross sections are found to be in striking agreement with Regge theory. The ρ and ω intercepts are found to be α_ρ=0.57 and α_ω=0.43. A comparison with forward nondiffractive cross sections verifies the ρ and ω Regge pole phases. The data are in strong agreement with universality, are compatible with exchange degeneracy, and indicate a substantial breaking of SU(3). Glauber screening corrections, with inelastic contributions added, are calculated and used to predict the total cross sections for scattering on deuterium. The predictions are in excellent agreement with the data.

I. Introduction

A new experiment[1] by Carroll et.al. at N.A.L. has yielded very precise values for the total cross sections for $\pi^{\pm}, K^{\pm}, p,$ and $\bar{p}$ on hydrogen and deuterium targets at four points in the momentum range $50 \leq p_{Lab} \leq 200$ GeV/c. For the first time a definite rise has been observed in all of the reactions except the $\bar{p}p$. The rise is especially dramatic in the K^+p cross section. Furthermore, the new data provide more exact and higher energy values for the differences of cross sections than have previously been available.

The purpose of this article is to phenomenologically analyze the high energy data available for hadron-hadron cross sections. In particular, our goals are (a) to parametrize the diffractive components of the cross sections as systematically and compactly as possible. (b) To determine whether the falling components of the cross sections are compatible with Regge theory. (c) To determine theoretically the screening corrections for scattering on deuterium and then compare the predicted deuterium cross sections with the data.

The plan of this article is as follows: In Chapter II we analyze the secondary (falling) components of the cross sections, which we find to be in striking agreement with Regge theory. In principle one would like to determine the residues and intercepts of the $f, \rho, \omega,$ and A_2 Regge trajectories directly by forming the linear combinations of cross sections which single out their contributions. This is not feasible in practice, however, because the uncertainties in the Glauber screening corrections needed to determine the neutron target cross sections are larger than many of the necessary cross section differences. Therefore, in Chapter II we limit our considerations to proton target reactions. We first fit the cross section differences $\Delta(\pi^+p)$, $\Delta(K^+p)$, and $\Delta(pp)$ to determine the ρ and ω intercepts (see Appendix A for notations),

yielding $\alpha_\rho = 0.57$ and $\alpha_\omega = 0.43$. The residues are shown to satisfy ω universality very precisely and to be compatible with ρ universality. Furthermore, the ω residue factorizes, indicating that the ϕ decouples from nucleons. On the other hand, an SU(3) prediction relating the couplings of the (non-degenerate) ρ and ω trajectories is substantially violated. It is shown that the very rapidly decreasing component of the pp difference can be represented by a threshold modification of the momentum parameter in the Regge power without invoking a low-lying supplementary trajectory. The falling components of the π^+p and pp cross sections are also analyzed although the actual parameters are dependent upon the functional form assumed for the diffractive component of the cross sections. The π^+p cross section supports f-ω exchange degeneracy and supports an SU(3) prediction relating the couplings of different particles to the same trajectory. The decreasing part of σ_{pp} is parametrized. It could be due to a small breaking of f-ω exchange degeneracy, a low lying singularity, or some other mechanism.

In Section II-B we predict the forward differential cross sections for various non-diffractive reactions using the parameters from II-A along with certain theoretical assumptions. We find virtually perfect agreement with experiment for the reactions $\pi^-p \to \pi^o n$ and $K_L^o p \to K_S^o p$, verifying our parameters and the Regge pole phase relations for the ρ and ω. Other reactions are found to be compatible with ρ-A_2 exchange degeneracy, although $\alpha_{A_2} < \alpha_\rho$ cannot be ruled out. Charge exchange reactions for which higher energy data would be especially useful are suggested.

In Chapter III we consider the diffractive (i.e. non-falling) components of the K^+p, π^+p, and pp cross sections. We find that the data are not sufficiently precise to distinguish between several different functional forms for the energy dependence. One particularly compact parametrization involves a

single logarithm.

$$\sigma_i^d(s) = C_i \ln\left(\frac{s + m_i}{b_i}\right) \qquad (1\text{-}1)$$

where σ_i^d is the diffractive cross section for particle i on protons, m_i is a "threshold" factor of order 1000 GeV^2, and b_i is a scale of order 1 GeV^2. The coefficients C_{K^+}, C_{π^+}, and C_p are successfully fixed in the ratio $1:1:\frac{3}{2}$, suggesting that if this parametrization holds true asymptotically, σ_{K^+p}, σ_{π^+p}, and σ_{pp} will all grow like ln s and be in the ratio $1:1:\frac{3}{2}$ (which is predicted by SU(3) and the naive quark model additivity assumption). The data are also successfully fit to other functional forms, such as

$$\sigma_i^d(s) = a_i + b_i \ln s + c_i \ln^2 s \qquad (1\text{-}2)$$

although no suggestive correlations between the parameters emerge. Unfortunately, the parameters of the falling components of the π^+p and pp cross sections are dependent upon which functional form is used for the diffractive component.

In Chapter IV we consider the deuterium target cross sections. At N.A.L. energies, the conventional elastic Glauber correction does not adequately represent the entire screening effect. Hence, in Chapter IV we determine the inelastic scattering contribution using available data on the inclusive reaction $pp \to pX$ (which is consistent with a nonvanishing triple Pomeranchukon coupling). The inelastic contribution is responsible for as much as 25% of the screening correction. We then combine our estimates of the screening corrections with the proton and neutron cross sections (the latter are computed assuming exchange degeneracy) to predict the deuteron target cross sections. The results are in excellent agreement with experiment.

Appendix A summarizes our conventions and notations, and Appendix B is a compendium of theoretical predictions for Regge parameters.

II Total Cross Section Differences and Secondary Regge Trajectories

In this chapter we describe our fits to the cross section differences $\Delta(\pi^+ p)$, $\Delta(K^+ p)$, and $\Delta(pp)$ and test various theoretical predictions concerning secondary trajectories.

A. Cross Section Differences

Consider first the ρ and ω trajectories. We have fit $\Delta(\pi^+ p)$ to a single power, the ρ (see Eqn. A5), with the result.

$$\begin{aligned} \beta^{\rho}_{\pi p} &= (2.62 \pm 0.05)\,mb \\ \alpha_{\rho} &= 0.574 \pm 0.01 \end{aligned} \tag{2-1}$$

The fit is displayed is Figure 1. The parameters of the fits are given in Table 1, and the extracted Regge parameters in Table 2.

$\Delta(K^+ p)$ involves two trajectories, the ρ and ω. It would be difficult to fit both simultaneously. Instead, we tentatively accept the ρ universality (or SU(3)) prediction (B6) to predict the ρ contribution from (2-1) and then fit the quantity

$$\Delta(K^+ p) - 2\beta^{\rho}_{Kp}\, p_{Lab}^{\alpha_\rho - 1} = 2\beta^{\omega}_{Kp}\, p_{Lab}^{\alpha_\omega - 1} \tag{2-2}$$

to determine the ω parameters. The excellent fit, which is shown in Figure 2, gives

$$\begin{aligned} \beta^{\omega}_{Kp} &= (7.95 \pm 0.13)\,mb \\ \alpha_{\omega} &= 0.433 \pm 0.01 \end{aligned} \tag{2-3}$$

The difference $\Delta(pp)$ involves not only the ρ and ω but also a component which falls rapidly (as $\sim p_{Lab}^{-1.5}$).

We have found that this falling component can be parametrized simply by writing

$$\Delta(pp) = 2\beta_{pp}^{\rho}\left(p_{Lab} - p_o\right)^{\alpha_\rho - 1} + 2\beta_{pp}^{\omega}\left(p_{Lab} - p_o\right)^{\alpha_\omega - 1} \qquad (2\text{-}4)$$

We tentatively use the universality conditions (B6) and (B7) to predict β_{pp}^{ρ} and β_{pp}^{ω} from (2-1) and (2-3) and perform a fit to determine p_o. The result is

$$p_o = (0.78 \pm 0.01)\ \text{GeV/c} \qquad (2\text{-}5)$$

which is a reasonable value for a threshold effect. The fit, shown in Figure 3, is remarkably successful. This is especially true when one considers that above 20 GeV/c Figure 3 is really a prediction, based on universality, from $\Delta(\pi^+ p)$ and $\Delta(K^+ p)$.

From the success of these fits we conclude that <u>ω universality</u>, $3\gamma_K^\omega = \gamma_p^\omega$, <u>is very accurate</u>, probably to better than 10%. Furthermore, <u>the ω residue factorizes</u>, indicating (a) it is really a pole, and (b) <u>that φ does in fact decouple from nucleons</u> (i.e. $\gamma_p^\phi \lesssim \gamma_K^\omega/10$).

The fits are also <u>compatible</u> with the ρ universality relations (B6), but since the ρ residues are so much smaller than the ω residues (Table 2), the fits to $\Delta(K^+ p)$ and $\Delta(pp)$ cannot be regarded as a sensitive test of (B6).

The ratio $\alpha_\rho/\alpha_\omega$ is given by

$$\frac{\alpha_\rho}{\alpha_\omega} = 1.32 \pm 0.04 \qquad (2\text{-}6)$$

<u>indicating a 30% breaking of the SU(3) prediction (B21)</u> ($\alpha_\rho = \alpha_\omega$ also follows from meson-meson exchange degeneracy (B4) when combined with (B1)).

Since $\alpha_\rho \neq \alpha_\omega$, any test of the SU(3) relation $\frac{1}{2}\gamma_\pi^\rho = \gamma_K^\omega$ (B20) is obscured by the ambiguity that the ratio $\frac{1}{2}\gamma_\pi^\rho/\gamma_K^\omega$ is dependent on the parameter s_o used to scale s in the Regge power. For $s_o = 2m_N \times 1\text{GeV}$ (which we have used),

$$\frac{\gamma_\pi^\rho}{2\gamma_K^\omega} = 0.70 \pm 0.01 \qquad (2\text{-}7)$$

while SU(3) predicts the ratio to be unity (B20). This indicates a 30% breaking of the SU(3) prediction for the factorized residues and a 50% breaking in the SU(3) predictions for the full residues. Had we used $s_o = 1 GeV^2$, the ratio (2.7) would be around 0.64.

We now turn to the f and A_2 trajectories and the question of exchange degeneracy. We shall see in Chapter IV that the ρ-A_2 exchange degeneracy predictions

$$\sigma_{K^+p} = \sigma_{K^+n}$$
$$\sigma_{pp} = \sigma_{pn} \qquad (2\text{-}8)$$

are compatible with the data. However, from Table 2 we see that the ρ (and A_2) contribution to these cross sections is insignificant compared to the ω (and f) contribution. Hence, the success of (2-8) is almost automatic at reasonably high energies.

The second prediction, that σ_{K^+p} and σ_{pp} should have no falling components, is much more stringent because it tests f-ω exchange degeneracy as well as ρ-A_2. The K^+p cross section shows no hint of a falling component above 3GeV/c. However, there is a quite substantial drop in σ_{pp} (about 9mb between $p_{Lab}=2.0$ and $p_{Lab}=50$ GeV/c). Unfortunately, due to the rising component in σ_{pp} it is impossible to uniquely determine the energy dependence of this falling component. If we parametrize this component as $\beta_{pp}\, p_{Lab}^{\alpha_{pp}-1}$, the data are compatible with any value of α_{pp} between 0.3 and 0.5. A "best fit" yields

$$\beta_{pp} = (11.1 \pm 0.3)\ mb$$
$$\alpha_{pp} = 0.42 \pm 0.05 \qquad (2\text{-}9)$$

(The details are described in Chapter III).

There are several possible explanations for this component; it could be the effect of a cut or of a low lying trajectory. It is probably not due to the f' or ϕ not decoupling, as a large effect would then be expected in σ_{K^+p} (see (B20) and (B23)). The (somewhat uncertain) value of α_{pp} in (2-9) suggests a breaking of

f-ω exchange degeneracy. If this were the case, and if the breaking were due entirely to the residues, then to account for

$$\beta_{pp} = (\gamma_p^f)^2 - (\gamma_p^\omega)^2 = 11.1 \text{ mb} \tag{2-10}$$

we require (Table 2)

$$\frac{\gamma_p^f}{\gamma_p^\omega} \simeq \frac{5.9}{4.9} = 1.2 \tag{2-11}$$

Such a 20% breaking is not unreasonable. However, in order to avoid the detection of a falling component in σ_{K^+p}, the exchange degeneracy relation $\gamma_K^f=\gamma_K^\omega$ would have to be reasonably well satisfied (or perhaps even $\gamma_K^f < \gamma_K^\omega$).

In the next chapter we describe our determination of

$$\beta_{\pi p}^f = \gamma_\pi^f \gamma_p^f = (16.8 \pm 0.8) \text{ mb} \tag{2-12}$$

The fit successfully assumes $\alpha_f=\alpha_\omega$.

If one assumes f-ω exchange degeneracy, then one expects $\gamma_p^f=\gamma_p^\omega$ and $\gamma_K^f=\gamma_K^\omega$. Furthermore, SU(3) predicts $\gamma_\pi^f=2\gamma_K^f$. (Here there is no scale ambiguity of the type found in comparing $1/2\ \gamma_\pi^\rho$ with γ_K^ω). Hence, the theoretical prediction (which also assumes factorization and $\beta_{\pi p}^{f'}=0$) is

$$\beta_{\pi p}^f \underset{SU(3)}{=} 2\beta_{Kp}^f \underset{f\text{-}\omega}{=} 2\beta_{Kp}^\omega = (15.9 \pm 0.3) \text{ mb} \tag{2-13}$$

in excellent agreement with (2-12).

On the other hand, the ρ-f exchange degeneracy relation (B5) (which requires a theoretical extension of duality ideas to unmeasured meson-meson amplitudes) predicts

$$\beta_{\pi p}^f \underset{\substack{\rho\text{-}f \\ f\text{-}\omega}}{=} \gamma_\pi^\rho \gamma_p^\omega = (11.1 \pm 0.1) \text{ mb} \tag{2-14}$$

Observe that the ρ-f relation suffers from the same scale ambiguity that was encountered in (2.7).

Of course, both (2-13) and (2-14) would have to be modified if (2-11) were true. However, (2-13) depends only on the product $\gamma_K^f\gamma_p^f$, which cannot differ

very much from β^{ω}_{Kp} because of the behavior of σ_{K^+p}.

Some possible tests of ρ-A_2 exchange degeneracy are described in Section B.

B) Charge and Isospin Exchange Cross Sections

In this section we predict the values of the forward differential cross sections for various nondiffractive reactions in terms of the Regge parameters determined from $\Delta(\pi p)$ and $\Delta(Kp)$. Our motivation is to test various aspects of Regge theory, such as the Regge phase, ρ-A_2 exchange degeneracy, and SU(3), as well as to further test the parameters of our fits. The predictions are compared with experiment and further experimental work is suggested.

1) $\pi^- p \to \pi^0 n$

The amplitude for $\pi^- p$ charge exchange is

$$T_{\pi^- p \to \pi^0 n} = \frac{1}{\sqrt{2}}\left(T_{\pi^+ p \to \pi^+ p} - T_{\pi^- p \to \pi^- p} \right) \qquad (2\text{-}15)$$
$$= -\sqrt{2}\, \beta^{\rho}_{\pi p} \left(\tan\frac{\pi\alpha_\rho}{2} + i \right) p_{Lab}^{\alpha_\rho}$$

Using Eqn. (A2) the forward differential cross section is

$$\left(\frac{d\sigma}{dt}\right)_0 = \frac{2}{16\pi}\left(\beta^{\rho}_{\pi p}\right)^2 \left[1 + \tan^2\left(\frac{\pi\alpha_\rho}{2}\right)\right] p_{Lab}^{2\alpha_\rho - 2} \qquad (2\text{-}16)$$
$$= 1.83\, p_{Lab}^{-.852}\ mb\,(GeV)^{-2}$$

where we have used the ρ parameters from Table 2. Comparison with experiment is complicated by the fact that the ρ coupling to nucleons is primarily of the helicity flip type[5], so the differential cross section dips in the forward direction. Nevertheless, the comparison of (2-16) with the experimental data in Figure 4 is dramatically successful; this supports not only the ρ parameters (Table 2) but also the phase relation (A3) which is appropriate to a Regge pole.

Hence, there is no need to introduce Regge cuts[7] as had been motivated by earlier experiments[8] which suggested $\alpha_\rho \sim 0.7$. Our value for α_ρ also agrees with the value 0.56 ± 0.10 recently determined[9] from the reaction $\pi^+ p \to \omega \Delta^{++}$.

2) $K_L^o p \to K_S^o p$

The regeneration amplitude is given by

$$T_{K_L^o p \to K_S^o p} = \frac{1}{2}\left[T_{K^o p \to K^o p} - T_{\bar{K}^o p \to \bar{K}^o p}\right] \qquad (2.17)$$
$$= \beta^{\rho}_{Kp}\left(\tan\frac{\pi\alpha_\rho}{2} + i\right) p_{Lab}^{\alpha_\rho} - \beta^{\omega}_{Kp}\left(\tan\frac{\pi\alpha_\omega}{2} + i\right) p_{Lab}^{\alpha_\omega}$$

Combining Eqn. (A2) and (2-17) with the Regge fit parameters in Table 2, we predict both the forward differential cross section and the phase ϕ of the forward amplitude $T_{K_L^o p \to K_S^o p}$. The results are compared with experiment in Figures 5 and 6. Again, the agreement is excellent. This verifies the parameters and Regge phase relation for the ω, which strongly dominates the amplitude. ($\beta^{\omega}_{Kp}/\beta^{\rho}_{Kp} = 6.1$). Incidentally the ω is largely helicity nonflip[5], so the cross section peaks in the forward direction.

3) $\pi^- p \to \eta n$

The reaction $\pi^- p \to \eta n$ should be dominated by the A_2 trajectory. Assuming ρ-A_2 exchange degeneracy,

$$\gamma^{A_2}_{pn} = \sqrt{2}\,\gamma^{A_2}_{p} = \sqrt{2}\,\gamma^{\rho}_{p} \qquad (2\text{-}18)$$
$$\alpha_\rho = \alpha_{A_2}$$

The π^--η-A_2 coupling is predicted by the SU(3) relation (B23)

$$\gamma^{A_2}_{\pi^-\eta} = \frac{2}{\sqrt{3}}\,\gamma^{A_2}_{K} = \frac{2}{\sqrt{3}}\,\gamma^{\rho}_{K} \qquad (2\text{-}19)$$

Since (2-19) relates couplings of the same trajectory to different particles, there is no scale ambiguity. Hence (using an even signature factor)

$$T_{\bar{\pi}p\to\eta n} = 2\sqrt{\tfrac{2}{3}}\,\beta^{S}_{Kp}\left(-\cot\tfrac{\pi\alpha_S}{2}+i\right)p_{Lab}^{\alpha_S} \qquad (2\text{-}20)$$

and

$$\left(\frac{d\sigma}{dt}\right)_0 = .381\; p_{Lab}^{-.852}\quad mb\,(GeV)^{-2} \qquad (2\text{-}21)$$

To make contact with experiment (in which the two photon decay of the η is measured), we multiply (2-21) by $\Gamma_{\eta\to 2\gamma}/\Gamma_{tot}$ =0.38 to obtain

$$\left(\frac{d\sigma}{dt}\right)_0 = .145\; p_{Lab}^{-.852}\;\mu b\,(GeV)^{-2} \qquad (2\text{-}22)$$

Comparison with experiment is again complicated by the forward dip of the cross section, but the agreement shown in Figure 7 is quite good above 4 GeV/c, supporting exchange degeneracy, SU(3), the A_2 Regge phase, and the ρ universality prediction of γ_K^ρ. Of course the data are also compatible[13] with $\alpha_{A_2}<\alpha_\rho$, so higher energy experiments would be quite useful.

4) $K^-p\to\bar{K}^0n$ and $K^+n\to K^0p$.

These reactions are a stringent test of ρ-A_2 exchange degeneracy as well as the value of β^ρ_{Kp}. The amplitudes are

$$T_{K^-p\to\bar{K}^0n} = T_{K^-n\to K^-n} - T_{K^-p\to\bar{K}^-p} = -2\left(T^S_{Kp}+T^{A_2}_{Kp}\right) \qquad (2\text{-}23)$$

and

$$T_{K^+n\to K^0p} = T_{K^+p\to K^+p} - T_{K^+n\to K^+n} = -2\left(T^S_{Kp}-T^{A_2}_{Kp}\right) \qquad (2\text{-}24)$$

where

$$T^{\rho}_{Kp} = \beta^{\rho}_{Kp} \frac{1 - e^{-i\pi\alpha_\rho}}{\sin\pi\alpha_\rho} p_{Lab}^{\alpha_\rho}$$

$$T^{A_2}_{Kp} = \beta^{A_2}_{Kp} \frac{-1 - e^{-i\pi\alpha_{A_2}}}{\sin\pi\alpha_{A_2}} p_{Lab}^{\alpha_{A_2}} \qquad (2\text{-}25)$$

If ρ-A_2 exchange degeneracy is valid, the differential cross sections should be equal for all (small) values of t. This seems roughly true experimentally[5,14] for $p_{Lab} \gtrsim 5$, but not for smaller p_{Lab}. The forward cross sections (which are again hard to measure because of the sharp forward dip) are predicted to be

$$\left(\frac{d\sigma}{dt}\right)_0 = \frac{1}{\pi}\left(\frac{\beta^{\rho}_{Kp}}{\sin\pi\alpha_\rho}\right)^2 p_{Lab}^{2\alpha_\rho - 2} \qquad (2\text{-}26)$$

$$= 1.49\, p_{Lab}^{-.852}\ mb(GeV)^{-2}$$

Equation (2-26) is compared with experiment in Figure 8. The agreement is good above 4 GeV/c except for the two highest energy points.[17] Earlier fits to the low energy data[18] have generally assumed broken ρ-A_2 exchange degeneracy to account for the non-equality of the K^-p and K^0n t distributions.

The rapid fall off of the cross section suggested by the last two points would be hard to understand on the basis of broken exchange degeneracy and might require strong absorption effects. Higher energy experiments on $K^-p \to \bar{K}^0n$ to settle these issues are clearly desirable.

5) $\bar{p}p \to \bar{n}n$ and $pn \to np$

The amplitudes

$$T_{\bar{p}p\to\bar{n}n} = T_{\bar{p}p\to\bar{p}p} - T_{\bar{p}n\to\bar{p}n}$$

$$T_{pn\to np} = T_{pp\to pp} - T_{pn\to pn} \qquad (2\text{-}27)$$

should also be dominated by the ρ and A_2. If this were true the differential cross sections should be equal for all small t, should exhibit forward dips, and (with ρ universality) the forward cross sections should be given by Eqn. (2-26). In fact, however, the cross sections show a forward peak, are much larger than Eqn. (2-26), and the forward cross section falls with an effective intercept around zero. The data and the prediction from (2-26) are shown in Figure 9. The standard explanation [21] for what is happening is that the cross section is being dominated by the pion trajectory and a scalar conspirator. What we wish to point out here is that for $p_{Lab} \gtrsim 100$ GeV/c the pion contribution to the cross section should be overwhelmed by the ρ-A_2 part (see Figure 9). The two highest energy points [22] may already be an indication of this. A higher energy experiment would be very desirable, not only to test ρ-A_2 exchange degeneracy but also to obtain β_{pp}^{ρ}.

III. The Total Cross Sections

The experimental results of Ref. (1) show that, with the exception of antiprotons, all total cross sections of hadrons on protons eventually grow with energy. For the first time a clear increase has been observed in $\pi^{\pm}p$, $\pi^{\pm}D$, $K^{-}p$ and $K^{-}D$ total cross sections. In addition, the accuracy of measurements in Ref. (1) is sufficient to begin a phenomenological examination of the way in which the cross sections increase.

To facilitate discussion, we will deal here with the total cross sections for pp, $\pi^{+}p$, and $K^{+}p$ interactions. From relatively low energy experiments it is clear that, beyond the resonance region, the pp and $\pi^{+}p$ cross sections fall substantially, while the $K^{+}p$ cross section does not. Regge theory attributes the falloff of the $\pi^{+}p$ cross section to the ρ and f trajectories, while the absence of a sharp falloff in the $K^{+}p$ cross section comes from the exchange degeneracy of the f and ω, ρ and A_2 trajectories (see Eqns. A-5). The low energy falloff of the pp cross section is not well understood, and may result from a breaking of exchange degeneracy, a lower lying singularity, or some other mechanism. Above 50 GeV/c, all three total cross sections begin to grow with energy, with the $K^{+}p$ cross section increasing sharply at lower energies, as shown in Figures 10-12.

Following the scheme outlined above, we parametrize the total cross sections with the general form

$$\begin{aligned} \sigma_{K^+p} &= D_{Kp} \\ \sigma_{\pi^+p} &= D_{\pi p} + \beta^{f}_{\pi p}\, p_{Lab}^{\alpha_f - 1} - \beta^{g}_{\pi p}\, p_{Lab}^{\alpha_g - 1} \\ \sigma_{pp} &= D_{pp} + B_{pp}\, p_{Lab}^{-n} \end{aligned} \qquad (3\text{-}1)$$

The values of $\beta_{\pi p}^{\rho}$ and α_ρ are taken directly from the difference measurements of $\Delta(\pi p)$, and the intercept α_f is taken to be the ω intercept, determined from the $\Delta(Kp)$ measurements as described in Chapter 2. In each reaction, D_{ip} is the diffractive component of the total cross section,[23] the object of primary interest, which contains the increasing part of the cross section for each reaction. The additional term included in σ_{pp} to account for the low energy falloff has β_{pp} and n as free parameters in the fit. One can successfully fit the pp data without such a term using, for example, $\sigma_{pp}=a_i+b_i[\ln(\frac{p_{Lab}}{c_i})]^{\alpha_i}$ with the low energy falloff of σ_{pp} coming from this diffractive term (see Table 3). However, we will also investigate strictly increasing diffractive terms, for which an additional non-diffractive term is necessary for σ_{pp}. Thus, we choose a strategy which maintains exchange degeneracy in the K^+p reaction, and we include the additional non-diffractive term in σ_{pp}.

The results of the fitting analysis show the total cross section data to be compatible with a number of functional forms for the diffractive components. Diffractive components such as[24] $D_{ip}=a_i+b_i \ln p_{Lab}+c_i(\ln p_{Lab})^2$, $D_{ip}= a_i+b_i(\ln p_{Lab})^{c_i}$ and $D_{ip}=C_i \ln[(p_{Lab}+m_i)/b_i]$ all give reliable fits to the cross section data (see Table 3). It is clear from this analysis that the experimental data are not measured to high enough energies or sufficient accuracy to single out one parametrization over all others.

We investigate further the parametrization[25]

$$D_{ip} = C_i \ln\left(\frac{P_{Lab} + m_i}{b_i}\right) \qquad (3\text{-}2)$$

Using this parametrization along with Eqns. (3-1) involves making a three parameter fit to the K^+p cross section, a four parameter fit to the π^+p cross section, and a five parameter fit to the pp cross section. This parametrization is fairly sensitive to the coefficients C_i for each reaction, and it is

found that a reliable fit to the data can be made with $C_K:C_\pi:C_p$ in the ratio $1:1:\frac{3}{2}$. The ratio $\frac{C_K}{C_\pi}=1$ suggests that SU(3) arguments may hold for the coefficients C_i, while the ratio $C_K:C_\pi:C_p$ of $1:1:\frac{3}{2}$ would be expected from extending the naive quark model to the coefficients. Taking the overall normalization of the C_i from the pp cross section gives the parametrization (26)

$$\sigma_{K^+p} = 3.27 \ln\left(\frac{P_{Lab}+149}{.80}\right)$$

$$\sigma_{\pi^+p} = 3.27 \ln\left(\frac{P_{Lab}+206}{.33}\right) + \frac{16.8}{P_{Lab}^{.567}} - \frac{2.62}{P_{Lab}^{.426}} \qquad (3\text{-}3)$$

$$\sigma_{pp} = 4.91 \ln\left(\frac{P_{Lab}+541}{.30}\right) + \frac{11.1}{P_{Lab}^{.58}}$$

where σ_{ip} are in millibarns and p_{Lab} is in GeV/c. These fits are illustrated by the solid curves in Figures 10-12. The parametrization of the data is not particularly sensitive to the values of m_i and b_i. By a small adjustment of C_i in each reaction, reliable fits may be made with m_i and b_i varying considerably. It can be concluded, however, that the scale b_i corresponds to a scale (in units of s) of $s_o \simeq 1\text{-}2\,(\text{GeV})^2$, which is a reasonable value for the energy scale. In addition, the fits indicate that the threshold parameter m_i increases as one goes from K^+p to π^+p to pp reactions. This gives a phenomenological mechanism for the faster growth of the K^+p cross section at low energies. If such a parametrization holds true, all the total cross sections will grow asymptotically as a single power (30) of $\log(p_{Lab})$, with σ_{K^+p} and σ_{π^+p} approaching each other, and both approaching 2/3 σ_{pp} asymptotically, as predicted by the naive quark model (Eqn. B-30).

An interesting result of the parametrization of $\sigma_{\pi^+ p}$ is the extraction of $\beta^f_{\pi p}$, a free parameter in the fit. While the value of the parameter depends on the functional form chosen for the diffractive component, the form of Eqn. (3-2) results in the value $\beta^f_{\pi p} = (16.8 \pm 0.8)$ mb. This is in close agreement with the value $2\beta^{\omega}_{Kp} = (15.9 \pm 0.25)$mb extracted from $\Delta(\pi p)$ and $\Delta(Kp)$ as described in Chapter 2.

The extraction of the non-diffractive component in σ_{pp} is again dependent on the form chosen for the pp diffractive term, as can be seen from Table 3. For the diffractive form of Eqn. (3-2), we find n=.58, a value quite close to that of the f-ω intercept. However, even with the particular diffractive form we have chosen, reliable fits can be found with n ranging from .5 to .8, by changing β_{pp}, C_p, m_p, and b_p appropriately.

In conclusion, it should be stressed that the total cross section data admit to a number of possible parametrizations with different diffractive components. While the parametrization discussed here appears to represent the diffractive component of total cross sections in a unified and theoretically appealing way, it is by no means unique. At this time, our parametrization should be considered a reasonable interpolation of the data.

IV Deuteron Screening and Total Cross Sections on Deuterium Targets

Until now we have considered only proton target cross sections. The reason for this is that the conventional elastic Glauber correction needed to extract neutron cross sections from the deuterium data is not sufficiently reliable at high energies: the inelastic rescattering corrections become important.(31-33)

In this chapter we will calculate the screening corrections, which constitute a sensitive test of the small t behavior of the data for the inclusive reaction $pp \to p+X$ and of the nonvanishing of the triple Pomeranchukon coupling.

Using the calculated screening corrections and the neutron target cross sections (which are predicted from exchange degeneracy), we then predict the deuteron target cross sections and compare them with the data. Our goal is to test the inelastic Glauber theory, as the uncertainties in this are larger than the effects of a small breaking of exchange degeneracy. It should be noted that the relations $\sigma_{-pn} = \sigma_{pp}$ and $\sigma_{K^+n} = \sigma_{K^+p}$ follow from ρ-A_2 exchange degeneracy alone. Since the ρ and A_2 couple relatively weakly (Table 2), any breaking of ρ-A_2 exchange degeneracy is irrelevant for our present purposes in the N.A.L. energy range. The predictions for σ_{K^-n} and σ_{-pn} require f-ω exchange degeneracy, which was seen to be generally compatible with the data in Chapter II. A small breaking would again be irrelevant here. The πn cross sections are related by isospin to the πp cross sections in Eqn. (A-5).

The total cross section for particle i on deuterium is

$$\sigma_{iD} = \sigma_{ip} + \sigma_{in} - \delta_i \qquad (4\text{-}1)$$

where δ_i is the Glauber screening correction. We will assume that the amplitudes are purely imaginary, which is an excellent approximation at N.A.L. energies.(34)

The Glauber correction can be written

$$\delta_i = \delta_i^{el.} + \delta_i^{inel.} \tag{4-2}$$

where δ_i^{el} is the elastic correction and δ_i^{inel} is the contribution from diffractively produced higher mass intermediate states.[32] The elastic contribution is given by

$$\delta_i^{el} = \frac{\sigma_{ip}\,\sigma_{in}}{8\pi\,(R^2 + b_i)} \tag{4-3}$$

We have chosen a Gaussian form for the deuteron form factor, $\exp(-R^2 \underset{\sim}{q}^2)$ with $R^2 = 37\ \text{GeV}^{-2}$ (see Ref. 32); b_i is the elastic slope.

The inelastic correction can be computed from a knowledge of the diffractive part of the inclusive cross section $i+p \to p+X$ and is very sensitive to the small t-behavior of this cross-section. In the triple-Regge model, a non-vanishing triple Pomeranchukon vertex is expected to give important contributions to δ_i^{inel}. Recently, high precision data have become available from the $p+D \to D+X$ experiment[35] at N.A.L., which show that up to $|t| = 0.03\ (\text{GeV})^2$ there is no indication of the vertex starting to vanish. From these data, the $p+p \to p+X$ cross-section has been extracted and parametrized by Goulianos[36] in the following form:

$$\frac{d\sigma_i}{dt\,dM^2} = \frac{A_i}{M^2}\, B\, e^{Bt} \tag{4-4}$$

where

$$B = 6\left[1 + \frac{0.06}{\left(M^2 - 1.35\right)^2 + 0.02}\right] (\text{GeV})^{-2} \tag{4-5}$$

and $A_{i=p} = 0.7$ mb. One can easily recognize that the parametrization (4-4) becomes the triple-Pomeranchukon expression for large values of the missing mass M and has the property of taking properly into account the correct t dependence for

small missing masses.

Using (4-4), the inelastic correction reads[32]

$$\delta_p^{inel} = 2A_p \int_{M_o^2}^{\infty} \frac{B\, e^{-\gamma^2(M^2 - m_p^2)^2}}{R^2+B} \frac{dM^2}{M^2} \qquad (4\text{-}6)$$

where $\gamma = m_D R/s$ ($s \approx 2m_p p_{Lab}$), and m_p and m_D are the proton and deuteron masses. δ_p^{inel} has been evaluated numerically taking $M_o^2 = 1.7(GeV)^2$. Typical values for δ_p^{inel} are 0.48 mb at 50 GeV/c and 0.75 mb at 200 GeV/c. As the elastic correction is $\delta_p^{el} \sim 3$ mb, we see that the inelastic contribution is substantial (as much as 25% of δ_p). We will assume $\delta_p^{inel} = \delta_{\bar{p}}^{inel}$ (as is appropriate in the triple Pomeranchukon region), take[37] $b_p \approx b_{\bar{p}} \approx 11.3(GeV)^{-2}$, and use the parametrizations for σ_{pp} and $\sigma_{\bar{p}p}$ obtained in Chapter 2 and 3 along with exchange degeneracy to compute $\sigma_{\bar{p}D}$ and σ_{pD}. The resulting cross-sections are compared with the experimental data in Figure 13. We consider the agreement between the theoretical predictions and the experimental data to be remarkable.

Since there are no available data for the inclusive processes $\pi^+ p \to p+X$ or $K^+ p \to p+X$ at small t values we will make the following approximations in order to compute δ_π^{inel} and δ_K^{inel}: a) start the integration in (4-6) at $M_o^2 = 5(GeV)^2$ in order to get rid of the small masses, since in this region the triple-Pomeranchukon picture is not expected to be valid (the reader should keep in mind that the calculation is very sensitive to the t dependence). Take

$$A_\pi = \frac{\sigma_{\pi p}}{\sigma_{pp}} A_p \simeq \frac{24}{38} A_p \quad , \quad A_K = \frac{\sigma_{Kp}}{\sigma_{pp}} A_p \simeq \frac{18}{38} A_p \qquad (4\text{-}7)$$

in Eq. (4-4). This approximation has been checked by computing the inclusive distribution in the high missing mass region for the $\pi^- p \to p+X$ experiment[38] at 205 GeV/c and good agreement was found. b) Use the estimate of the A_1 enhancement of Rf. 33. (one gets $\simeq$ 0.12 mb) as representing the contribution of

the small missing masses; we have arbitrarily taken 0.08 mb for the small mass region contribution to the Kp→p+X reaction. Since the elastic slopes are not known in the NAL range, we have left b_π and b_K in Eq.(4-3) as free parameters and have determined them through a best fit to the K^+D and $\pi^\pm D$ cross sections. Therefore our results for δ_K and δ_π are not entirely predictions; however the sensitivity of (4-3) to the exact values of b_π and b_K is small. The values obtained are $b_\pi = 6(\text{GeV/c})^{-2}$ and $b_K = 9.5(\text{GeV/c})^{-2}$. The value obtained for b_π is somewhat smaller than would have been guessed from the lower energy data ($\approx 8.5(\text{GeV})^{-2}$). The errors in our estimate of δ_π^{inel} and in our parametrizations could account for the difference.

The computed cross sections for $\pi^\pm D$, $K^- D$, and $K^+ D$ are shown in Figures 14 and 15 along with the experimental data. The agreement is again excellent, although the prediction for $\sigma_{K^- D}$ is slightly higher than the two highest energy data points.

We consider the agreement between theory and experiment for the deuteron cross sections to be a very strong confirmation of the theory of inelastic screening corrections[31-33] and of the inclusive data[35] which indicates a nonvanishing triple-Pomeranchukon vertex.

Finally, we consider $\Delta(K^+D)$ and $\Delta(pD)$. From Equations (4-1) and (A-5) we have

$$\Delta(K^+D) = 4 B^{\omega}_{Kp} \left(1 - \frac{D_{Kp}}{8\pi(R^2 + b_K)}\right) \equiv 4 \xi_K B^{\omega}_{Kp} \tag{4-8}$$

and

$$\Delta(pD) = 4 B^{\omega}_{pp} \left(1 - \frac{D_{pp}}{8\pi(R^2 + b_p)}\right) \equiv 4 \xi_p B^{\omega}_{pp} \tag{4-9}$$

where we have neglected a very small term proportional to $(B^{\omega})^2$. Neglecting the energy dependence of D_{Kp} and D_{pp} (a second order effect), the energy dependence of $\Delta(K^+D)$ and $\Delta(pD)$ is predicted to be $p_{Lab}^{\alpha_\omega - 1}$, which is in complete agreement with the data.

Using the data for σ_{K^+p} and σ_{pp} in the 50-200 GeV/c range[1] we predict from (4-8) and (4-9):

$$\xi_K = 0.96 \pm 0.01$$
$$\xi_p = 0.92 \pm 0.01 \qquad (4\text{-}10)$$

We have fit $\Delta(K^+D)$ and $\Delta(pD)$ using the values for α_ω and $\beta_{pp}^{\omega} = 3\beta_{Kp}^{\omega}$ from Table 2. For $\Delta(pD)$, p_{Lab} was replaced by $p_{Lab} - p_o^D$, where p_o^D was fit in order to describe the very low energy behavior correctly. The result is

$$\xi_K = 0.90 \pm 0.01$$
$$\xi_p = 0.87 \pm 0.01 \qquad (4\text{-}11)$$
$$p_o^D = (0.94 \pm 0.02)\ \text{GeV/c}$$

The details of the fit are given in Table 1. The agreement between (4-10) and (4-11) is reasonable, especially when one considers that $\Delta(K^+D)$ and $\Delta(pD)$ are small quantities. They are very sensitive to systematic errors in the data and to the approximations made for the screening corrections.

We conclude therefore that ω universality ($\beta_{pp}^{\omega} = 3\beta_{Kp}^{\omega}$) and the screening corrections in Equation (4-8) and (4-9) are valid to around 5%.

V. Conclusion

We have analyzed and fit the available data on the total cross sections of $\pi^{\pm}$,$K^{\pm}$,p, and $\bar{p}$ on protons. The resulting parameters were used to predict the forward differential cross sections for several non-diffractive reactions, and the predictions were compared with experiment. The (inelastic) Glauber screening corrections for the scattering of pions, kaons, and nucleons on deuterium were determined; the corrections, when combined with proton target cross sections, were used to predict the deuteron target cross sections, which were then compared with experiment.

Our conclusions are: (a) the diffractive components of the cross sections are compatible with several different functional forms for the energy dependence. (b) One very compact parametrization predicts that the K^+p, π^+p, and pp cross sections will all rise asymptotically as ln s. The coefficients will be in the ratio 1:1:$\frac{3}{2}$ predicted by SU(3) and the naive quark model. (c) The parameters of the falling components of σ_{π^+p} and σ_{pp} depend on the functional form of the diffractive component. (d) ω universality is satisfied extremely well, while ρ universality is compatible with the data. (e) Factorization is successful, the ϕ decouples from nucleons, and the data supports $\beta_{\pi p}^{f'}=0$. (f) The amplitude phases predicted by Regge theory for the ρ and ω are correct. (g) SU(3) relations between the residues of non-degenerate trajectories are substantially violated, while SU(3) relations involving the same trajectory are compatible with the data. (h) f-ω exchange degeneracy is supported by the data, although the falling component of σ_{pp} could indicate a small breaking. (i) ρ-A_2 exchange degeneracy is compatible with the data, but further experiments are required. (j) ρ-f exchange degeneracy for residues appears violated, but the test is dependent on the parametrization of the diffractive component of σ_{π^+p}. (The predictions for secondary trajectories can be summarized as follows: all lines in Figure B connecting the f-ω complex to the ρ-A_2 complex are violated. Lines within the f-ω and the ρ-A_2

complexes are supported by or compatible with the data). (k) The inelastic contributions to the Glauber screening corrections, computed using inclusive scattering data which suggest a nonvanishing triple Pomeranchukon coupling, are substantial (up to 25% of the entire correction). (l) The deuteron cross sections which are predicted (assuming f-ω and ρ-A_2 exchange degeneracy as well as the computed screening corrections), are in excellent agreement with the data.

Acknowledgement

It is a pleasure to thank K. Goulianos, H. Sticker, and H. Pagels for very useful discussions. We are especially indebted to R.L. Cool for a great deal of help and advice.

Appendix A. Notation and Conventions

Our amplitudes T(s,t) are normalized so that the total cross section is

$$\sigma_{ab}(s) = \frac{1}{p_{Lab}} \, Im\, T_{ab\to ab}(s,0) \tag{A1}$$

where $p_{Lab} \approx s/2m_N$ is the laboratory momentum in GeV/c. A differential cross section is given by

$$\frac{d\sigma}{dt} = \frac{1}{16\pi} \, \frac{|T|^2}{p_{Lab}^2} \tag{A2}$$

We denote the diffractive component of the total cross section, which we assume is an isosinglet, by $D_{ab}(s)$.

The contribution of a normal Regge pole with trajectory $\alpha_i(t)$ to $T_{ab\to ab}$ is given by

$$\beta_{ab}^i(t) \left(\frac{\mp 1 - e^{-i\pi\alpha_i}}{\sin\pi\alpha_i} \right) p_{Lab}^{\alpha_i} \tag{A3}$$

where the minus (plus) sign applies to even (odd) signature trajectories. The residue β_{ab}^i factorizes:

$$\beta_{ab}^i = \gamma_a^i \, \gamma_b^i \tag{A4}$$

If a or b is a Fermion, (A4) is true for each helicity amplitude. At t=0, however, only the helicity non-flip amplitude survives.

We are mainly interested here in the f,f' ρ,ω,ϕ, and A_2 trajectories, all of which have intercepts near 1/2. Their properties are listed in Table A. It is generally believed[5] that the ϕ and f' decouple from nucleons.

The total cross sections of interest here are

$$\begin{aligned}
\sigma_{\pi^- p} &= D_{\pi p} + B^f_{\pi p} + B^s_{\pi p} \\
\sigma_{\pi^+ p} &= D_{\pi p} + B^f_{\pi p} - B^s_{\pi p} \\
\sigma_{\pi^- n} &= \sigma_{\pi^+ p} \\
\sigma_{\pi^+ n} &= \sigma_{\pi^- p}
\end{aligned} \tag{A5}$$

$$\sigma_{K^-p} = D_{Kp} + B^{f}_{Kp} + B^{s}_{Kp} + B^{\omega}_{Kp} + B^{A_2}_{Kp}$$
$$\sigma_{K^+p} = D_{Kp} + B^{f}_{Kp} - B^{s}_{Kp} - B^{\omega}_{Kp} + B^{A_2}_{Kp}$$
$$\sigma_{K^-n} = D_{Kp} + B^{f}_{Kp} - B^{s}_{Kp} + B^{\omega}_{Kp} - B^{A_2}_{Kp}$$
$$\sigma_{K^+n} = D_{Kp} + B^{f}_{Kp} + B^{s}_{Kp} - B^{\omega}_{Kp} - B^{A_2}_{Kp}$$
$$\sigma_{\bar{p}p} = D_{pp} + B^{f}_{pp} + B^{s}_{pp} + B^{\omega}_{pp} + B^{A_2}_{pp}$$
$$\sigma_{pp} = D_{pp} + B^{f}_{pp} - B^{s}_{pp} - B^{\omega}_{pp} + B^{A_2}_{pp}$$
$$\sigma_{\bar{p}n} = D_{pp} + B^{f}_{pp} - B^{s}_{pp} + B^{\omega}_{pp} - B^{A_2}_{pp}$$
$$\sigma_{pn} = D_{pp} + B^{f}_{pp} + B^{s}_{pp} - B^{\omega}_{pp} - B^{A_2}_{pp}$$

where $B^{i}_{ab} \equiv \gamma^{i}_{a}\gamma^{i}_{b}\, p_{Lab}^{\alpha_i - 1}$. Of course, lower lying trajectories should in principle be added to (A5). The f'(ϕ) trajectories, if present, would enter (A5) with the same signs as the f(ω).

We shall sometimes use the notation

$$\Delta(ab) \equiv \sigma_{\bar{a}b} - \sigma_{ab} \qquad \text{(A6)}$$

Appendix B. Compendium of Theoretical Predictions for Regge Residues

In this Appendix we summarize[39] various theoretical predictions concerning the couplings of secondary Regge poles ($f, f', \rho, \omega, \phi, A_2$) to pions, kaons, and nucleons. We concentrate on three major ideas: 1) Exchange degeneracy, which relates the couplings of odd signature vector trajectories to those of even signature tensor trajectories. 2) ρ and ω universality, which relates the couplings of vector mesons to pions, to kaons, and to nucleons. 3) SU(3), which relates the couplings of different particles and trajectories within SU(3) multiplets. The different classes of predictions are summarized in Figure B .

Several comments are in order: a) To aid in making reliable tests, predictions are generally expressed in terms of factorized Regge residues rather than as sums or differences of total cross sections. b) The major predictions of higher symmetries, such as SU(6), are generally equivalent to the union of SU(3) with universality. c) As the data seem to be in striking agreement with Regge theory, we do not consider quark model additivity predictions, except when they are expressible in Regge language. d) Most of the predictions can be straightforwardly generalized to include hyperon-baryon and strangeness exchange cross sections.[40]

1) Exchange Degeneracy[41-44]

Exchange degeneracy comes in two forms. Weak exchange degeneracy predicts that pairs of opposite signature trajectories should be equal (e.g. $\alpha_\rho(t) = \alpha_{A_2}(t)$), while strong exchange degeneracy further asserts that the residues are equal (e.g. $\beta^{\rho}_{Kp}(t) = \beta^{A_2}_{Kp}(t)$). The "modern" theoretical motivation for exchange degeneracy is as follows: 1) assume the existence of finite energy sum rules

(without wrong signature fixed poles) for full scattering amplitudes (which are not of definite signature). 2) Adopt the Harari-Freund ansatz:[45] the direct channel resonances are dual to secondary Regge trajectories while the nonresonant background is dual to the Pomeronchukon singularity (diffraction). 3) Hence, for channels which are exotic (no direct channel resonances) the secondary Regge trajectories must cancel. This requires the equality of both the trajectory functions and residues of pairs of opposite signature Regge poles.

The predictions based upon the experimentally accessible meson-baryon and baryon-baryon amplitudes are:

$$\begin{aligned} \alpha_\rho &= \alpha_{A_2} \\ \alpha_f &= \alpha_\omega \\ \alpha_{f'} &= \alpha_\varphi \end{aligned} \tag{B1}$$

and

$$\begin{aligned} \gamma_p^\rho &= s_1 \gamma_p^{A_2} \\ \gamma_K^\rho &= s_1 \gamma_K^{A_2} \\ \gamma_p^f &= s_2 \gamma_p^\omega \\ \gamma_K^f &= s_2 \gamma_K^\omega \\ \gamma_p^{f'} &= s_3 \gamma_p^\varphi \\ \gamma_K^{f'} &= s_3 \gamma_K^\varphi \end{aligned} \tag{B2}$$

where $s_1 s_2$, and s_3 are ± 1. Equations (B1) and (B2) should also apply for $t \neq 0$ (the predictions for the baryon residues then apply to each spin amplitude separately).

Equations (B1) and (B2) are equivalent to

$$\sigma_{K^+p} = \sigma_{K^+n} = D_{Kp}$$
$$\sigma_{pp} = \sigma_{pn} = D_{pp} \tag{B3}$$

That is, these cross sections should have no $1/s^{1/2}$ parts.(46)

If one further speculates that the duality arguments apply to meson-meson amplitudes, one can also predict

$$\alpha_\rho = \alpha_f \tag{B4}$$

and

$$\gamma_\pi^f = g_4 \gamma_\pi^\rho$$
$$\gamma_K^f = g_4 \gamma_K^\rho \tag{B5}$$
$$\gamma_\pi^{f'} = 0$$

For such theoretical developments of exchange degeneracy as bootstraps, the prediction of higher symmetries from SU(3) and exchange degeneracy, ideal nonet mixing angles, and the necessary failure of the Harari-Freund ansatz for antibaryon-baryon channels, we refer the reader to Ref. (42)-(44) and references therein.

2) Universality(47-49)

ρ universality is the prediction

$$\frac{1}{2}\gamma_\pi^\rho = \gamma_K^\rho = \gamma_p^\rho \tag{B6}$$

at t=0, while ω universality states

$$\gamma_K^\omega = \frac{1}{3}\gamma_p^\omega \tag{B7}$$

It is implicit in (B7) that

$$\gamma_p^\varphi = 0 \tag{B8}$$

Universality can be motivated in two ways: 1) In quark models, universality follows from the assumption that the ρ couples universally to the quark isospin current, and that the ω couples universally to the number of nonstrange quarks in the hadron.

2) Universality also is predicted by the union of vector-meson dominance with SU(3) (with ideal nonet mixing). This requires "smooth extrapolations" between the points $(1,0)$, $(1,m_\rho^2)$, and $(\alpha_\rho(0),0)$ in the (J,t) plane.

Equation (B6) implies

$$\Delta(\pi^+p) = \Delta(K^+p) - \Delta(K^+n) \tag{B9a}$$

$$= \Delta(pp) - \Delta(pn) \tag{B9b}$$

while (B7) implies

$$\Delta(pp) + \Delta(pn) = 3\left[\Delta(K^+p) + \Delta(K^+n)\right] \tag{B10}$$

(B9) and (B10) can be combined to yield a result independent of neutron targets:

$$\Delta(pp) = 3\Delta(K^+p) - \Delta(\pi^+p) \tag{B11}$$

Of course, low lying trajectories ($\alpha \lesssim 0$) should violate (B9)-(B11).

3) SU(3)

Consider the SU(3) invariant couplings[50-52] of an octet of pseudoscalar mesons ϕ_ℓ, $\ell=1\ldots8$, an octet of baryons ψ_ℓ, nine vector mesons v_ℓ, $\ell=0\ldots8$, and nine tensor meson t_ℓ. Defining the matrices

$$\begin{aligned} M &\equiv \frac{1}{\sqrt{2}} \sum_{\ell=1}^{8} \lambda_\ell \phi_\ell \\ B &\equiv \frac{1}{\sqrt{2}} \sum_{\ell=1}^{8} \lambda_\ell \psi_\ell \\ V &\equiv \frac{1}{\sqrt{2}} \sum_{\ell=0}^{8} \lambda_\ell v_\ell \\ T &\equiv \frac{1}{\sqrt{2}} \sum_{\ell=0}^{8} \lambda_\ell t_\ell \end{aligned} \tag{B12}$$

where $\lambda_0 \equiv \sqrt{\frac{2}{3}}\, I$, the most general invariant couplings are

$$L_{VMM} = \sqrt{2}\ \gamma_{MV}\ Tr\left(M[V,M]\right) \tag{B13}$$

which is pure f type ((Tr V)(Tr MM) is forbidden by charge conjugation)

$$\begin{aligned} L_{V\bar{B}B} = \sqrt{2}\,\gamma_{BV}\Big[& f_V\, Tr\left(\bar{B}[V,B]\right) \\ & + (1-f_V)\, Tr\left(\bar{B}\{V,B\}\right) \\ & + \beta\left(Tr\, V\right)\left(Tr\,\bar{B}B\right)\Big] \end{aligned} \tag{B14}$$

$$\begin{aligned} L_{TMM} = \sqrt{2}\,\gamma_{MT}\Big[& Tr\left(M\{T,M\}\right) \\ & + \varepsilon\left(Tr\,T\right)\left(Tr\,MM\right)\Big] \end{aligned} \tag{B15}$$

which is pure d type, and

$$\begin{aligned} L_{T\bar{B}B} = \sqrt{2}\,\gamma_{BT}\Big[& f_T\, Tr\left(\bar{B}[T,B]\right) \\ & + (1-f_T)\, Tr\left(\bar{B}\{T,B\}\right) \\ & + \delta\left(Tr\,T\right)\left(Tr\,\bar{B}B\right)\Big] \end{aligned} \tag{B16}$$

where γ_{MV}, γ_{BV}, γ_{MT}, γ_{BT}, f_V, f_T, β, ε, and δ are arbitrary constants.

The SU(3) predictions can be made in three stages: 1) With no assumptions concerning ϕ–ω and f–f' mixing, the only predictions of interest here are

$$\frac{1}{2}\,\gamma_\pi^g = \gamma_K^g \tag{B17}$$

and

$$\gamma_K^{A_2} = \frac{\sqrt{3}}{2}\,\gamma_{\pi^0\eta}^{A_2} \tag{B18}$$

Eqn. (B17), which also follows from ρ universality, leads immediately to (50) (B9a). 2) In the second stage one assumes ideal nonet mixing (52)

$$\begin{aligned} \omega &= \sqrt{\tfrac{1}{3}}\, v_8 + \sqrt{\tfrac{2}{3}}\, v_0 \\ \varphi &= \sqrt{\tfrac{2}{3}}\, v_8 - \sqrt{\tfrac{1}{3}}\, v_0 \\ f &= \sqrt{\tfrac{1}{3}}\, t_8 + \sqrt{\tfrac{2}{3}}\, t_0 \\ f' &= \sqrt{\tfrac{2}{3}}\, t_8 - \sqrt{\tfrac{1}{3}}\, t_0 \end{aligned} \tag{B19}$$

This ideal mixing, which is supported by the Gell-Mann Okubo formula, is suggested by the quark model: it corresponds to the ω and f being composed of nonstrange quarks only, while the φ and f' are composed of strange quarks only. Ideal mixing is also predicted by exchange degeneracy. In addition to (B18) one now has

$$\tfrac{1}{2}\gamma_\pi^\rho = \gamma_K^\rho = \gamma_K^\omega = \sqrt{\tfrac{1}{2}}\,\gamma_K^\varphi = \gamma_{MV} \tag{B20}$$

3) In the third step, one assumes $\gamma_\pi^{f'}=0$, (which is supported by the experimental fact that the f' does not decay into two pions and is predicted by exchange degeneracy), and $\gamma_p^{f'} = \gamma_p^{\phi}=0$, (which is supported by previous Regge fits). Both are predicted by the simple quark model, since the proton and pion are composed of nonstrange quarks only. It is also usual to assume SU(3) breaking in the sense that

$$\begin{aligned} \alpha_\rho = \alpha_\omega &\neq \alpha_\varphi \\ \alpha_{A_2} = \alpha_f &\neq \alpha_{f'} \end{aligned} \tag{B21}$$

which corresponds to giving the strange quark a different mass from the nonstrange quarks.

One now has (in addition to (B20))

$$\begin{aligned} \varepsilon &= 0 \\ \beta &= 2f_V - 1 \\ \delta &= 2f_T - 1 \end{aligned} \tag{B22}$$

and

$$\gamma_\rho^S = \frac{1}{4f_V - 1}\gamma_\rho^\omega = \gamma_{BV}$$

$$\frac{\sqrt{3}}{2}\gamma_{\pi^0\eta}^{A_2} = \gamma_K^{A_2} = \gamma_K^f = -\sqrt{\tfrac{1}{2}}\gamma_K^{f'} = \tfrac{1}{2}\gamma_\pi^f = \gamma_{MT} \qquad \text{(B23)}$$

$$\gamma_\rho^{A_2} = \frac{1}{4f_T - 1}\gamma_\rho^f = \gamma_{BT}$$

$$\gamma_\rho^g = \gamma_\rho^{f'} = \gamma_\pi^{f'} = 0$$

Of course, equations (B20), (B21) and (B23) can be extended to $t \neq 0$.

4) Combinations

By combining any two of exchange degeneracy, universality, and SU(3) much stronger predictions emerge. For example, ρ universality plus SU(3) predicts

$$\gamma_{MV} = \gamma_{BV} \qquad \text{(B24)}$$

while the further assumption of ω universality implies

$$f_V = 1 \qquad \text{(B25)}$$

From (B20), (B23) and (B25)((B24) is not required) one finds the Johnson-Treiman formulas[53]

$$\Delta(K^+p) = 2\Delta(K^+n) = 2\Delta(\pi^+p) \qquad \text{(B26)}$$

which were originally suggested by M(12) symmetry (which also yields $f_V = 1$). Adding the universality condition (B24), one obtains the Freund relation[54]

$$\Delta(pp) = \frac{5}{4}\Delta(pn) = 5\Delta(\pi^+p) \qquad \text{(B27)}$$

The combination of SU(3) with exchange degeneracy implies

$$
\begin{aligned}
f_V &= f_T \\
\beta &= \delta \\
\gamma_{MV} &= \pm \gamma_{MT} \\
\gamma_{BV} &= \pm \gamma_{BT} \\
\alpha_\rho &= \alpha_\omega = \alpha_f = \alpha_{A_2}
\end{aligned}
\tag{B28}
$$

If one combines SU(3), universality, and exchange degeneracy, then all of the couplings can be expressed in terms of $\gamma_{MV} = \gamma_K^\rho$, as illustrated in Figure B.

5) Diffraction

The assumption that the Pomeranchukon singularity is an SU(3) singlet implies

$$D_{\pi p} = D_{Kp} \tag{B29}$$

while the naive quark additivity assumption[55] implies

$$\frac{2}{3} D_{pp} = D_{\pi p} = D_{Kp} \tag{B30}$$

References

1) A. S. Carroll , Rockefeller University Preprints, COO-2232A-7,8.

2) ■ A. Citron et.al., Phys. Rev. 144, 1101 (1966); ✕ K.J. Foley et.al., Phys. Rev. Lett. 19, 330 (1967); ▲ S.P. Denisov et.al., Phys. Lett. 36B, 415 and 528 (1971) and Nucl. Phys. B65, 1(1973); ⊛ Carroll et. al., Ref.1.

3) ✕ W. Galbraith et.al., Phys. Rev. 138B, 913 (1965); ▲ Denisov et.al., Ref.2.; ● Carroll et.al., Ref.1; ■ R.J. Abrams et.al., Phys. Rev. D1, 1917 (1970).

4) ■ D.V. Bugg et.al., Phys. Rev. 146, 980 (1968) and Abrams, et.al., Ref.3; other symbols as in Ref.3.

5) Excellent references to previous Regge fits are P.D.B. Collins, Phys. Reports 1C, 103 (1971), and P.D.B. Collins and E.J. Squires, Regge Poles in Particle Physics, Springer-Verlag, Berlin and New York, 1968.

6) ● Wahlig et.al. 68, ■ Yvert 68, ◎ Mannelli et.al. 65, □ Guisan et.al. 71, ▲ Guisan et.al. 68, ✕ Bonamy et.al. 70, complete references in Particle Data Group Summary LBL-63 (1973); △ P. Sonderegger et.al., Phys. Lett. 20, 75 (1966) and A.V. Stirling et.al., Phys. Rev. Lett. 14, 763 (1965); ▽ V.N. Bolotov et.al, Phys. Lett. 38B, 120 (1971) and Serpukhov preprint IHEP 73-52 (1973).

7) R.W. Hanson, Phys. Rev. D5, 1227 (1972); V. Barger and R.J.N. Phillips, Nucl. Phys. B40, 205 (1972). The latter authors were aware that the discrepancy could be due to a scale error in Ref.8.

8) S.P. Denisov et. al., Ref.2.

9) W.F. Buhl et. al., Phys. Lett. 48B, 388 (1974).

10) ✕ Darriulat et.al. 70, ◎ Leipuner et.al. 63, □ Buchanan et.al. 71, △ Firestone et.al. 66, ■ Brody et. al. 71, complete references in Particle Data Group Summary LBL-55 (1972); ● G.W. Brandenburg et.al., Phys. Rev. D9, 1939 (1974); ▽ V.K. Birulev et.al., Phys. Lett. 38B, 452 (1972) and JINR preprint (1972).

11) We have adjusted the (transmission regeneration) cross sections of Darriulat, Buchanan, and Birulev in Ref.10 by the factor $|\eta_{+-}^{new}/\eta_{+-}^{old}|$, where $|\eta_{+-}^{new}|=(2.23\pm0.05)\times10^{-3}$, R. Messer et.al., Phys. Rev. Lett. 30, 876 (1973), and $|\eta_{+-}^{old}|$ is whatever value was used originally to normalize the experiment. This is a 10-15% effect and does not qualitatively alter Figure 5. We are indebted to H. Sticker for advice on this point.

12) ● V.N. Bololov et.al., Serpukhov preprint IHEP 73-57 (1973); ▣ O.Guisan et.al., Phys. Lett. 18, 200 (1965); ◎ Guisan, 71, from Ref.6.

13) V.N. Bolotov et.al., Ref. 12.

14) R. Diebold et.al., Phys. Rev. Lett. 32, 904 (1974).

15) ▽ Litchfield et.al. 71, + Moscoso et.al. 70, ✕ Astbury et.al. 66, ∧ Buffington et.al. 68, complete references in Compilation of Cross Sections, CERN/HERA 72-2 (1972); ▩ V.N. Bololov et.al., Serpukhov preprints IHEP 73-53 and 73-58 (1973); ▲ R. Diebold et.al., Ref. 14; ● M. Aguilar-Benitez et.al., Phys. Rev. D4, 2583 (1971); ▬ J. Badier et.al., CEA-R-3037(1966); ≪ R. Blokzijl et.al., Nucl. Phys. B51, 535 (1973); ✳ K.J. Foley et.al., Phys. Rev. D9, 42 (1974).

16) ▽ Butterworth et.al. 65, ▣ Firestone et.al. 70, complete references in Compilation of Cross Sections, op.cit., △ R. Diebold et.al. Ref.14; ◎ Y. Goldschmidt-Clermont et.al., Phys. Lett. 27B, 602 (1968); ▱ D. Cline et.al., Nucl. Phys. B22, 247 (1970).

17) V.N. Bolotov et.al., Ref. 15.

18) A. Derem and G. Smadja, Nuovo Cim. A62, 681 (1969); See also the complex Regge pole model of N. Barik and B.R. Desai, Phys. Rev. D6, 3192 (1972). Both references assume $\alpha_{A_2}<\alpha_\rho$.

19) ● Larsen 60, ▩ Shepard et.al. 69, ▲ Manning et.al. 66, complete references in Particle Data Group Summary UCRL-20000 NN (1970).

20) ◎ Atwood et.al. 70, ▣ Czyzewski et.al. 70, △ Astbury et.al. 66, complete references in Particle Data Group Summary LBL-58 (1972); ▽ V.N. Bolotov et.al., Serpukhov preprint IHEP 73-58 (1973).

21) R.J.N. Phillips, Nucl. Phys. B2, 394 (1967).

22) V.N. Bolotov et.al., Ref.20.

23) Some relevant review articles and theoretical papers on diffractive components are: F. Zachariasen, Physics Reports 2C, 1(1971), D. Horn and F. Zachariasen, Hadron Physics at Very High Energies, (Benjamin, 1973), P.V. Landshoff and J.C. Polkinghorne, Physics Reports 5C, 1(1972), V.N. Gribov, Soviet Physics JETP 26, 414 (1968), V.N. Gribov and A.A. Migdal, Soviet Journal of Nucl. Phys. 8, 583 & 703 (1969), V. Barger and R.J.N. Phillips, Nucl. Phys. B40, 205 (1972), H. Cheng, J.K. Walker, and T.T. Wu, Phys. Lett. 44B, 97 and 283 (1973).

24) Parametrizations of the form $D_{ab} = A + B(\ln p_{Lab})^2$ are theoretically questionable, since they implicitly set a scale of 1 GeV/c inside the logarithm. In general, such a scale factor should be fit to the data.

25) Examples of diffractive components increasing asymptotically as ln s exist in the literature. J.S. Ball and F. Zachariasen, Phys. Lett. 40B, 411 (1972), V. Barger & R.J.N. Phillips, Ref.23, and references therein.

26) The parametrization of σ_{K^+p}, σ_{π^+p} and σ_{pp} with $C_K : C_\pi : C_p$ in the ratio $1:1:\frac{3}{2}$ was motivated by a best fit to each reaction separately, which gave C_i values quite close to this ratio. The choice of a single power of ln p was motivated primarily by simplicity. One can reliably fit the cross section data with

$$D_{ip} = C_i \left[\ln\left(\frac{p_{Lab} + m_i}{b_i}\right)\right]^{\alpha_i}$$

with values of α_i ranging roughly from .5 to 1.5. The fit to the $\pi^+ p$ cross section data with (3-3) appears to be the least reliable of the fits, primarily because of the discrepancies among the low energy data points (see Fig. 11).

27) ▽ Galbraith et.al., Ref.3; ▲ Denisov et.al., Ref.2; ⊛ Carroll et.al., Ref.1.

28) ✕ Foley et.al., Ref.2; the other symbols are as in Ref. 27.

29) + S.R. Amendolia et.al., Phys. Lett. 44B, 119(1973), ■ U. Amaldi et.al, Phys. Lett. 44B, 112 (1973); ▼ Denisov et.al., Ref.2; ● Carroll et.al., Ref.1; ✕ Foley et.al., Ref.2; □ G. Bellettini et.al, Phys. Lett. 14, 164(1965). ○ D.V. Bugg et.al., Ref.4; △ J. Ginestet et.al., Nucl. Phys. B13, 283 (1969).

30) The asymptotic growth of the total cross sections as $\ln p_{Lab}$ is theoretically reasonable. So far, the only example of an amplitude with σ_t increasing and satisfying Mandelstam analyticity, $\pi\pi$ crossing symmetry, polynomial boundedness, and unitarity for each isospin amplitude, has $\sigma_t \sim \ln p_{Lab}$ asymptotically. J. Kupsch, Forschr. Phys. 19, 783 (1971).

31) Yu. P. Gorin et.al., Sov. Jour. Nucl. Phys. 15, 530 (1972).

32) C. Quigg and L.-L. Wang, Phys. Lett. 43B, 314 (1973) and references therein.

33) J. Kwiecinski, L. Lesniak, and K. Zalewski, Cracow preprint (1974).

34) We also ignore two body charge exchange corrections, C. Wilkin, Phys. Rev. Lett. 17, 561 (1966), which are negligible at N.A.L. energies.

35) Y. Akimov et.al., Rockefeller preprint COO-223AA-1, submitted to the Conference on High Energy Physics, London, July 1974.

36) K. Goulianos, private communication.

37) V. Bartenev et.al, Phys. Rev. Lett. 31, 1088 (1973).

38) D. Leith, AIP Conference Proceedings No. 14, p.349 (1974).

39) Our references concentrate on the original papers and on the papers which are currently the most useful.

40) Some predictions may be found in H.J. Lipkin, Phys. Rev. D7, 846(1973).

41) R.C. Arnold, Phys. Rev. Lett. 14, 657(1965).

42) H.J. Lipkin, Nucl. Phys. B9, 349 (1969).

43) J. Mandula, J. Weyers, and G. Zweig, Ann. Rev. Nucl. Sci. 20, 289 (1970).

44) M. Kugler, Proc. of the 9th Schladming School, 1970, P. Urban, ed. Springer-Verlag, Wien. p.443.

45) H. Harari, Phys. Rev. Lett. 20, 1395 (1968); P.G.O. Freund, Phys. Rev. Lett. 20, 235 (1968).

46) Whether lower lying trajectories should also cancel is an open question.

47) C.A. Levinson, N.S. Wall, and H.J. Lipkin, Phys. Rev. Lett. 17, 1122 (1966).

48) V. Barger, K. Geer, and F. Halzen, Nucl. Phys. B44, 475 (1972).

49) H.J. Lipkin, Phys. Rev. D5, 776 (1972).

50) V. Barger and M. Rubin, Phys. Rev. 140, B1365 (1965).

51) V. Barger and M. Olsson, Phys. Rev. 146, 1080 (1966).

52) V. Barger, M. Olsson, and K.V.L. Sarma, Phys. Rev. 147, 1115 (1966).

53) K. Johnson and S.B. Treiman, Phys. Rev. Lett. 14, 189 (1965).

54) P.G.O. Freund, Phys. Rev. Lett. 15, 929 (1965).

55) See, for example, J.J.J. Kokkedee, The Quark Model, W.A. Benjamin, Inc., New York and Amsterdam 1969, and references therein. Also, H.J. Lipkin WIS-74/17-Ph.

TABLE CAPTIONS

1. Fits to cross section differences. All momenta are in GeV/c, and $B^i_{ab} = \beta^i_{ab} P_{lab}^{\alpha_i - 1}$. χ^2/ν is the total chi-squared divided by the number of degrees of freedom. The errors given on the parameters have been determined by a standard least-squares fitting procedure for functions nonlinear in the coefficients. For practical purposes, such a determination tends to underestimate errors. See, for example, P.R. Bevington, Data Reduction and Error Analysis for the Physical Sciences, (McGraw-Hill, 1969)p.242.

2. Secondary Regge parameters determined from $\Delta(\pi^+ p)$, $\Delta(K^+ p)$, and $\Delta(pp)$. Also included are the parameters determined in Chapter III.

3. Parametrizations of σ_{K^+p}, σ_{π^+p}, and σ_{pp} using various diffractive forms. In cases 1)-3), the fits are made as described below Eqns. (3-1). In case 4), σ_{pp} is parametrized without a term $\beta_{pp}\, p_{Lab}^{-n}$. χ^2/ν given for each fit is the total chi-squared divided by the number of degrees of freedom.

A) Properties of the major Regge trajectories. The last column refers to the principle coupling to nucleons for $t \neq 0$.

Table 1

Quantity	Value	P_{lab} Range	number of points	χ^2/ν
$\Delta(\pi^+p)=cp_{Lab}^{-n}$	$c=(5.24\pm0.10)$mb $n=0.426\pm.01$	4.43-200	27	0.82
$\Delta(K^+p)-2B^{\rho}_{Kp}=cp_{Lab}^{-n}$	$c=(15.9\pm0.25)$mb $n=0.567\pm.01$	3-200	22	0.66
$\Delta(pp)=2\beta^{\rho}_{pp}(p_{Lab}-p_o)^{\alpha_\rho-1}+2\beta^{\omega}_{pp}(p_{Lab}-p_o)^{\alpha_\omega-1}$	$p_o=(0.78\pm0.01)$	2.75-200	23	0.65
$\Delta(K^+D)=4\xi_K B^{\omega}_{Kp}$	$\xi_K=0.90\pm0.01$	3.0 -200	22	0.84
$\Delta(pD)=4\xi_p\beta^{\omega}_{pp}(p_{Lab}-p_o^D)^{\alpha_\omega-1}$	$\xi_p=0.87\pm0.01$ $p_o^D=(0.94\pm0.02)$	2.50-200	24	0.83

Table 2

Quantity	Value	Comment
α_ρ	0.574±0.01	
α_ω	0.433±0.01	
$\frac{1}{2}\beta^\rho_{\pi p}=\beta^\rho_{Kp}=\beta^\rho_{pp}$	(1.31±0.03) mb	$\beta^\rho_{\pi p}$ determined from $\Delta(\pi^+ p)$
$\frac{1}{2}\gamma^\rho_\pi=\gamma^\rho_K=\gamma^\rho_p$	$(1.14\pm0.01)(\text{mb})^{\frac{1}{2}}$	
$3\beta^\omega_{Kp}=\beta^\omega_{pp}$	(23.9±0.4) mb	β^ω_{Kp} determined from $\Delta(K^+ p)$
$\gamma^\omega_p=3\gamma^\omega_K$	$(4.88\pm0.04)(\text{mb})^{\frac{1}{2}}$	
$\beta^f_{\pi p}$	(16.8±0.8) mb	assumes $\alpha_f=\alpha_\omega$
γ^f_π	$(3.44\pm0.18)(\text{mb})^{\frac{1}{2}}$	assumes $\gamma^f_p=\gamma^\omega_p$
α_{pp}	0.42±0.05	effective trajectory for σ_{pp} falloff from parametrization (3-2)
β_{pp}	(11.1±0.3) mb	effective residue for σ_{pp} falloff from parametrization (3-2)

Table 3: Parametrizations of Total Cross Sections

Reaction	K^+p	π^+p	pp
No. of Data Pts.	19	25	66
p_{Lab} Range	8-200 GeV/c	10-200 GeV/c	4.5-2000 GeV/c

1) Diffractive Term: $D_{ip} = C_i \ln\left(\frac{p_{Lab}+m_i}{b_i}\right)$

$C_i, \beta^f_{\pi p}, \beta_{pp}$ in millibarns; p_{Lab}, m_i, b_i in GeV/c

C_i=3.27±.07	C_i=3.27±.07	C_i=4.91±.11
m_i=149±7	m_i=206±23	m_i=541±54
b_i=.80±.03	b_i=.33±.02	b_i=.30±.06
χ^2/ν = .56	$\beta^f_{\pi p}$=16.8±.8	β_{pp}=11.1±.3
	χ^2/ν = 1.27	n = .58±.05
		χ^2/ν = .99

2) Diffractive Term: $D_{ip} = a_i + b_i \ln p_{Lab} + c_i (\ln p_{Lab})^2$

$a_i, b_i, C_i, \beta^f_{\pi p}, \beta_{pp}$ in millibarns; p_{Lab} in GeV/c

a_i=18.3±.3	a_i=14.4± 3.3	a_i=22.6±.9
b_i=-.98±.20	b_i=1.56± 1.08	b_i= -2.19±.34
c_i=.24±.03	c_i=0.0± 0.1	c_i=.41±.02
χ^2/ν = .45	$\beta^f_{\pi p}$=29.4± 5.1	β_{pp}=23.5±.9
	χ^2/ν =1.07	n = .07±.02
		χ^2/ν = 1.16

Table 3: Parametrizations (continued)

Reaction	K^+p	π^+p	pp

3) Diffractive Term: $D_{ip}=a_i+b_i(\ln p_{Lab})^{c_i}$

$a_i, b_i, \beta^f_{\pi p}, \beta_{pp}$ in millibarns; p_{Lab} in GeV/c.

$a_i=17.1\pm.1$	$a_i=11.2\pm3.2$	$a_i=7.65\pm.98$
$b_i=.01\pm.006$	$b_i=3.14\pm1.81$	$b_i=1.62\pm.26$
$c_i=3.35\pm.29$	$c_i=.76\pm.18$	$c_i=1.31\pm.06$
$\chi^2/\nu = .48$	$\beta^f_{\pi p}=32.2\pm2.8$	$\beta_{pp}=39.7\pm1.0$
	$\chi^2/\nu =1.07$	$n = .16\pm.10$
		$\chi^2/\nu = 1.70$

4) Diffractive Term: $D_{ip}= a_i+b_i[\ln(p_{Lab}/c_i)]^{d_i}$

$a_i, b_i, \beta^f_{\pi p}, \beta_{pp}$ in millibarns; p_{Lab}, c_i in GeV/c.

(NOTE: σ_{pp} is fit without a term $\beta_{pp}\, p_{Lab}^{-n}$ in this case)

$a_i=17.3\pm.1$	$a_i=21.8\pm.3$	$a_i=38.3\pm.1$
$b_i=.23\pm.28$	$b_i=.49\pm.09$	$b_i=.44\pm.05$
$c_i=7.6\pm6.5$	$c_i=27.7\pm5.7$	$c_i=63.2\pm1.5$
$d_i=2.02\pm.64$	$d_i=1.53\pm.25$	$d_i=2.02\pm.09$
$\chi^2/\nu =.48$	$\beta^f_{\pi p}=5.8\pm2.1$	$\chi^2/\nu = 1.13$
	$\chi^2/\nu = 1.09$	

Table A

Trajectory	I^G	C	Signature	Coupling
f	0^+	+	even	non-flip
f′	0^+	+	even	-
ρ	1^+	-	odd	flip
ω	0^-	-	odd	non-flip
φ	0^-	-	odd	-
A_2	1^-	+	even	flip

Figure Captions

1) $\Delta(\pi^+p) = \sigma_{\pi^-p} - \sigma_{\pi^+p}$. The details of the fit to the ρ are described in Tables 1 and 2. The data are from Ref. 2.

2) $\Delta(K^+p) = \sigma_{K^-p} - \sigma_{K^+p}$ fit to determine the ω parameters. The ρ parameters are taken from the fit to $\Delta(\pi^+p)$, and the fit is described in Tables 1 and 2. The data are from Ref. 3.

3) $\Delta(pp) = \sigma_{\bar{p}p} - \sigma_{pp}$ fit to $2\beta^{\rho}_{pp}(p_{Lab} - p_o)^{\alpha_\rho - 1} + 2\beta^{\omega}_{pp}(p_{Lab} - p_o)^{\alpha_\omega - 1}$. The residues are predicted from $\Delta(\pi^+p)$ and $\Delta(K^+p)$ and the fit is to p_o. The details are in Tables 1 and 2 and the data are from Ref. 4.

4) $(d\sigma/dt)_o$ for $\pi^-p \to \pi^0 n$. The line is the prediction (2.16). The data are from Ref. 6.

5) $(d\sigma/dt)_o$ for $K^0_L p \to K^0_S p$ compared with the prediction from (2.17). The data are from Ref. 10. See also the note in Ref. 11.

6) The phase of the forward amplitude for $K^0_L P \to K^0_S P$, compared with the prediction from (2.17). The data are from Ref. 10.

7) $(d\sigma/dt)_o$ for $\pi^-p \to \eta n \to 2\gamma + n$. The line is the prediction (2.22). The data are from Ref. 12.

8) $(d\sigma/dt)_o$ for $K^-p \to \bar{K}^0 n$ (solid points) and $K^+n \to K^0p$ (open points) compared with the prediction (2.26). The data are from Ref. 15 (K^-p) and Ref. 16 (K^+n).

9) $(d\sigma/dt)_o$ for $pn \to np$ (solid points) and $\bar{p}p \to \bar{n}n$ (open points) compared with the ρ-A_2 contribution predicted from Eqn. (2.26). The data are from Ref. 19 (pn) and Ref. 20 ($\bar{p}p$).

10) σ_{K^+p}. The curve is the result of the fit (3-3) and the data are from Ref. 27.

11) σ_{π^+p}. The curve is the fit (3-3) and the data are from Ref. 28.

12) σ_{pp}. The curve is the fit (3-3) and the data are from Ref. 29.

13) $\sigma_{\bar{p}D}$ upper curve and σ_{pD} lower curve. The data are from Denisov et. al, Ref. 2 and Carroll et.al., Ref. 1. The curves represent the predicted cross-sections.

14) $\sigma_{\pi^\pm D}$. Same as in Fig. 13.

15) σ_{K^-D} upper curve and σ_{K^+D} lower curve. Same as in Fig. 13.

B) Theoretical predictions for secondary Regge residues.

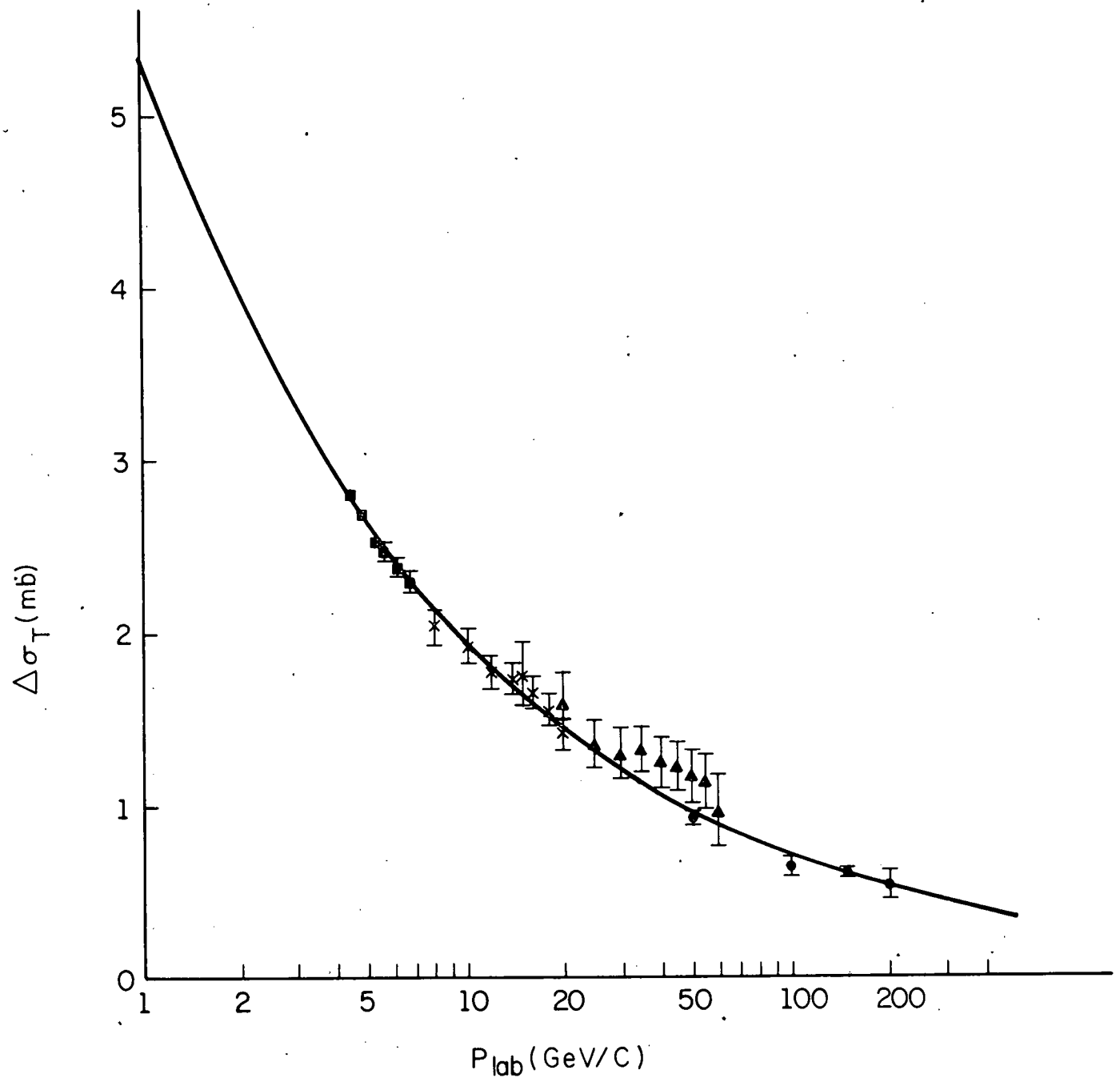

Figure 1

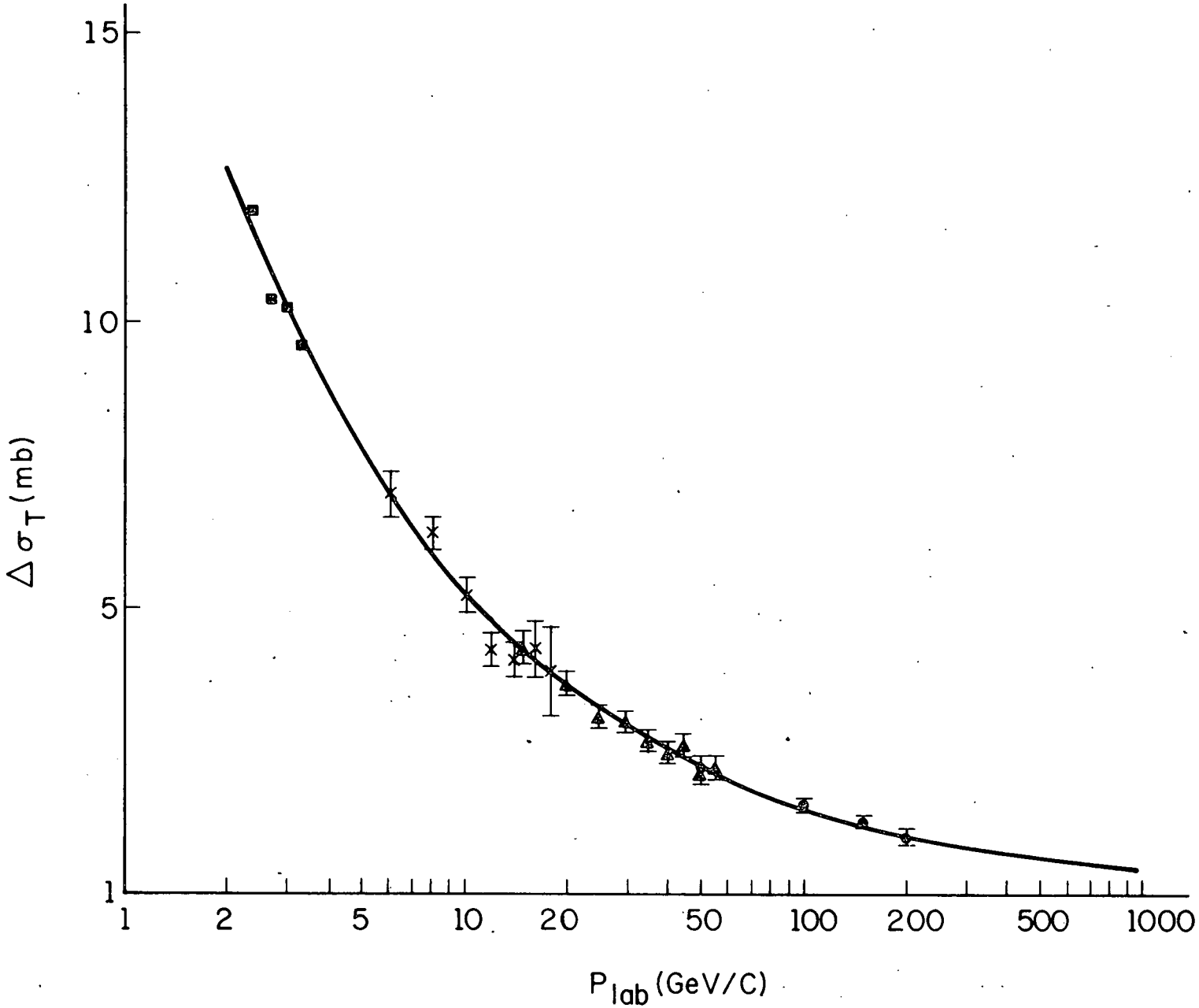

Figure 2

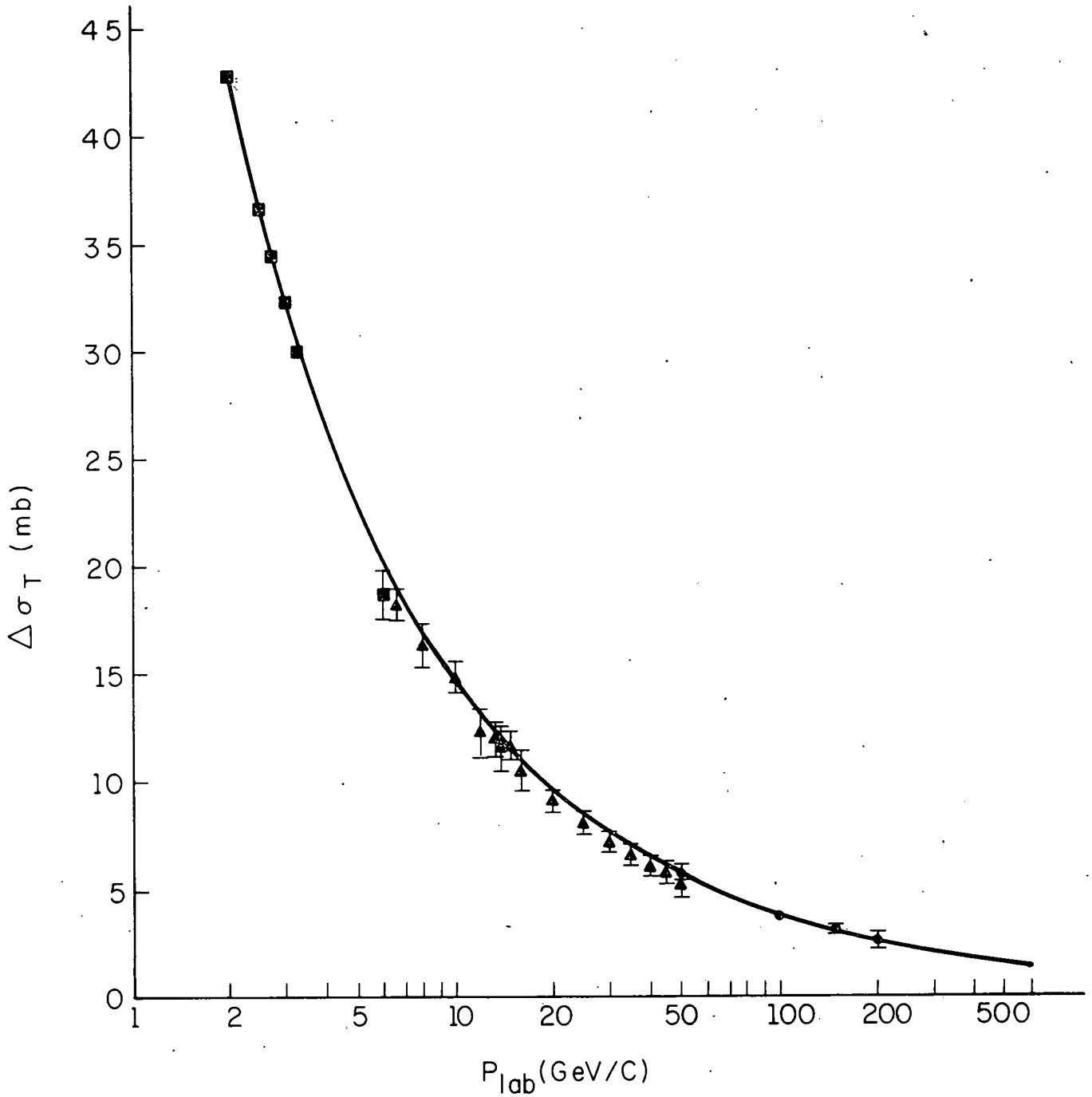
45
40
35
30
25
20
15
10
5
0
$\Delta\sigma_T$ (mb)
1
2
5
10
20
50
100
200
500
P_{lab}(GeV/C)

Figure 3

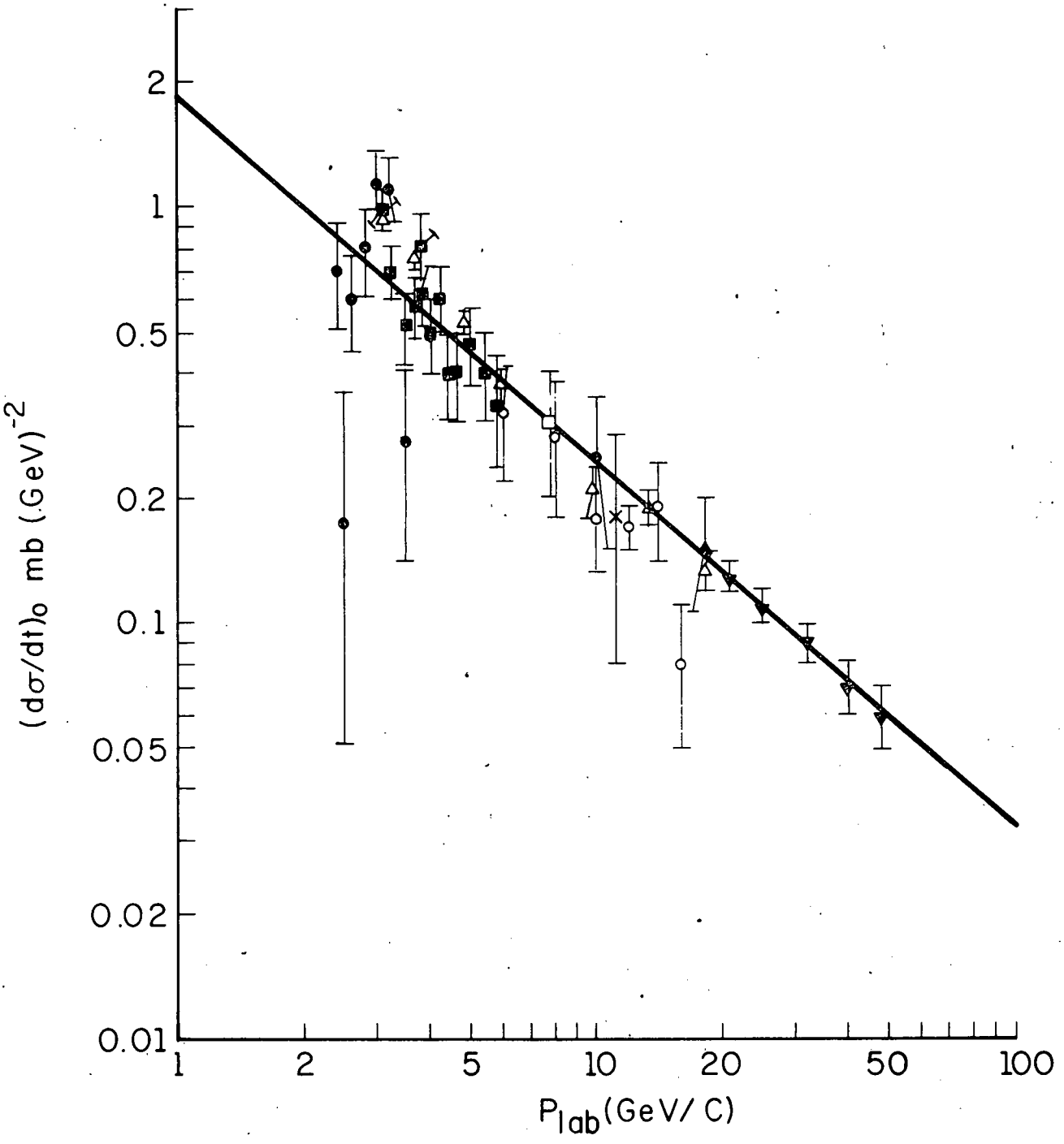
2
1
0.5
0.2
0.1
0.05
0.02
0.01
$(d\sigma/dt)_0$ mb (GeV)$^{-2}$
1
2
5
10
20
50
100
P_{lab}(GeV/C)

Figure 4

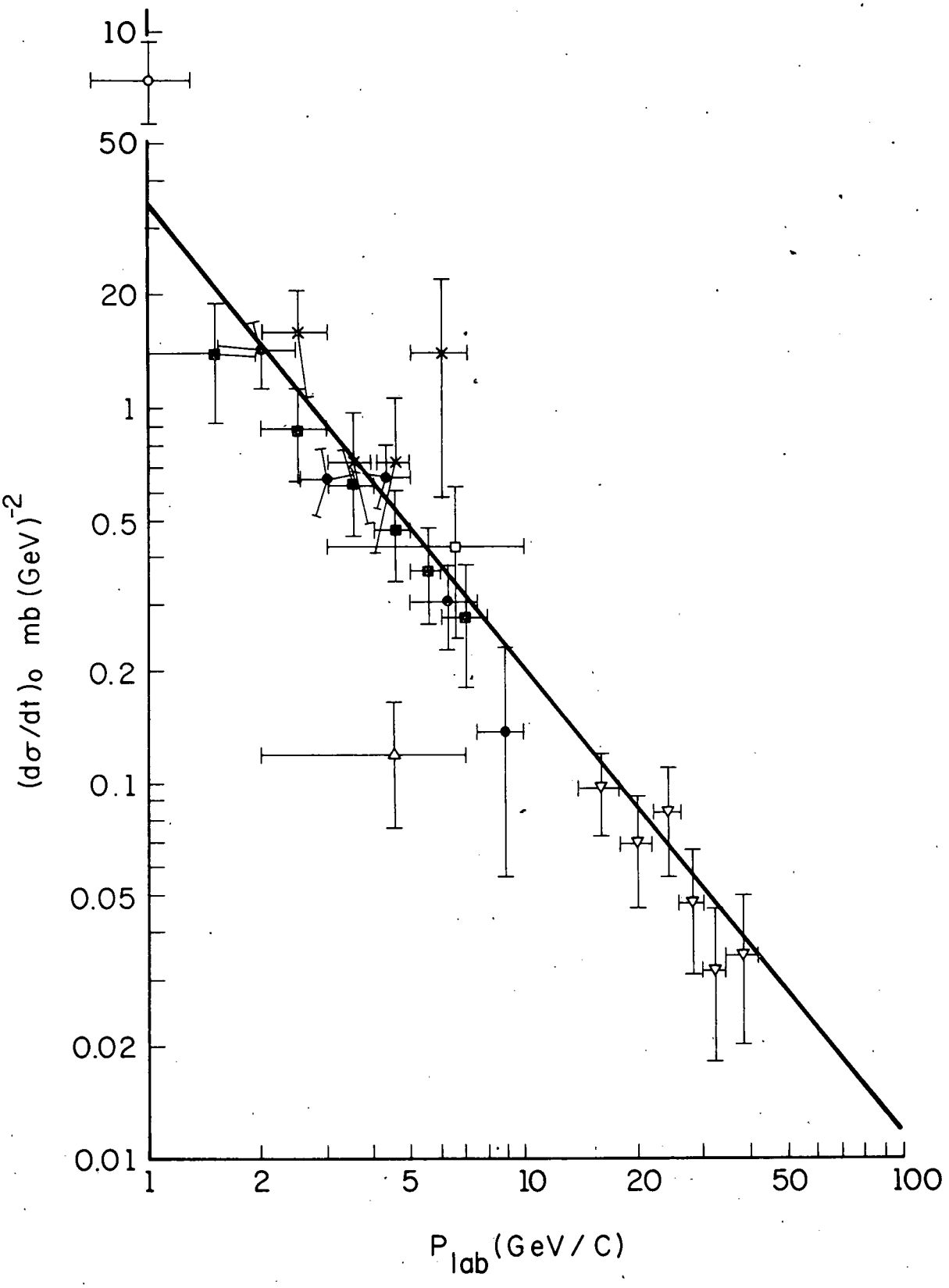
10
50
20
1
0.5
0.2
0.1
0.05
0.02
0.01
$(d\sigma/dt)_o$ mb (GeV)$^{-2}$
1
2
5
10
20
50
100
P_{lab} (GeV/C)

Figure 5

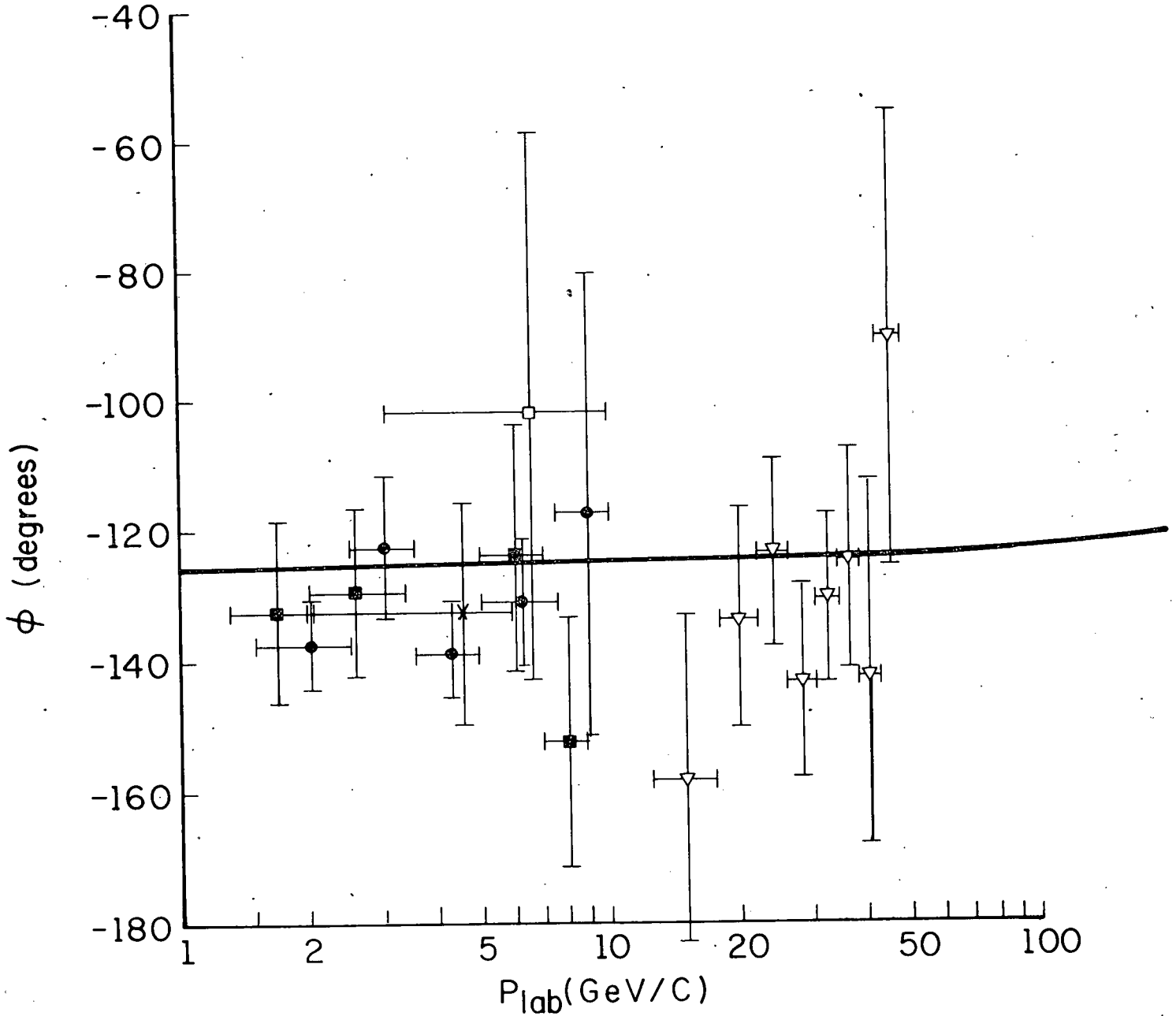

Figure 6

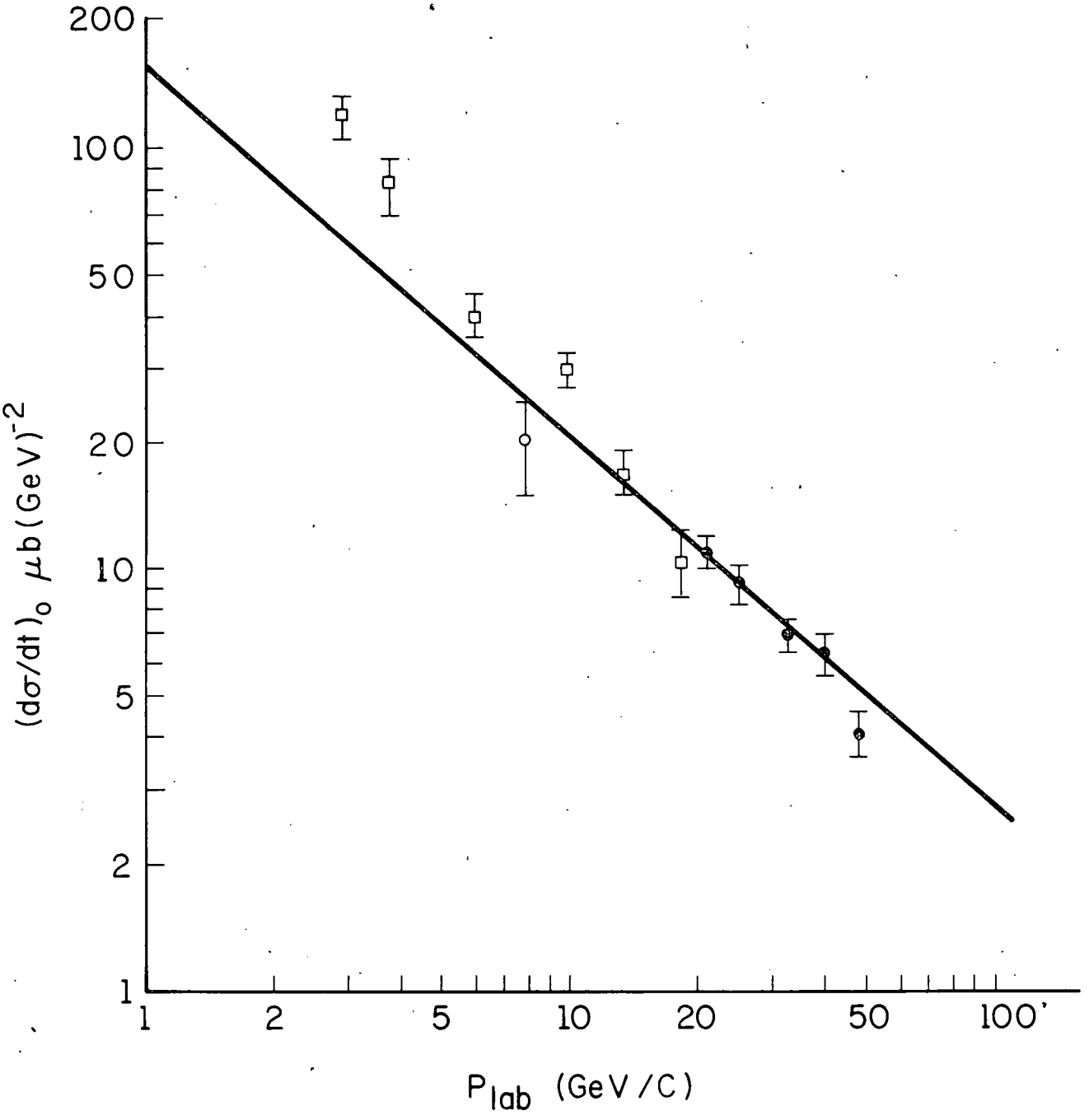
200
100
50
20
10
5
2
1
1
2
5
10
20
50
100
$(d\sigma/dt)_o$ $\mu b\,(GeV)^{-2}$
P_{lab} (GeV/C)

Figure 7

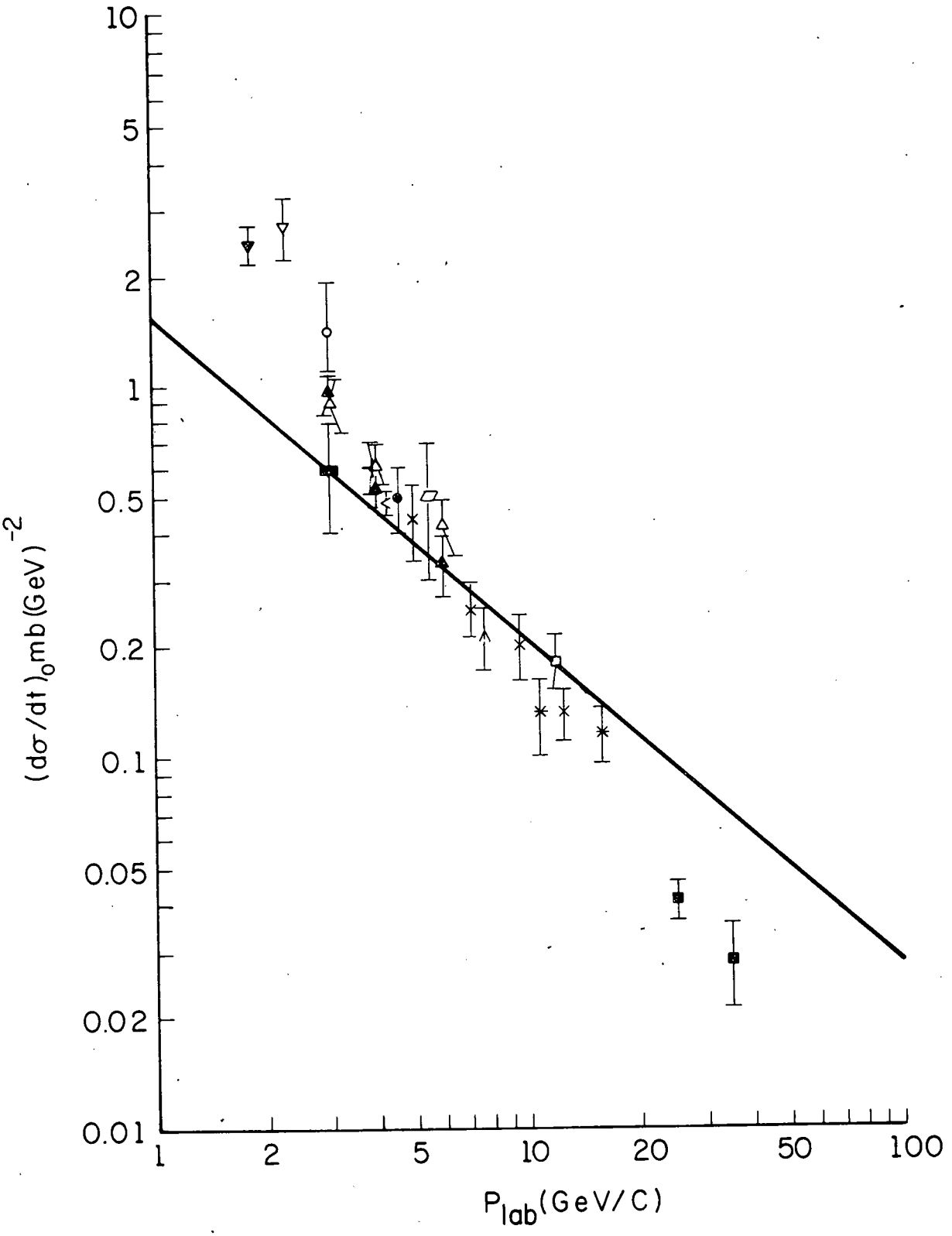
10
5
2
1
0.5
0.2
0.1
0.05
0.02
0.01
1
2
5
10
20
50
100
$(d\sigma/dt)_0 mb(GeV)^{-2}$
$P_{lab}(GeV/C)$

Figure 8

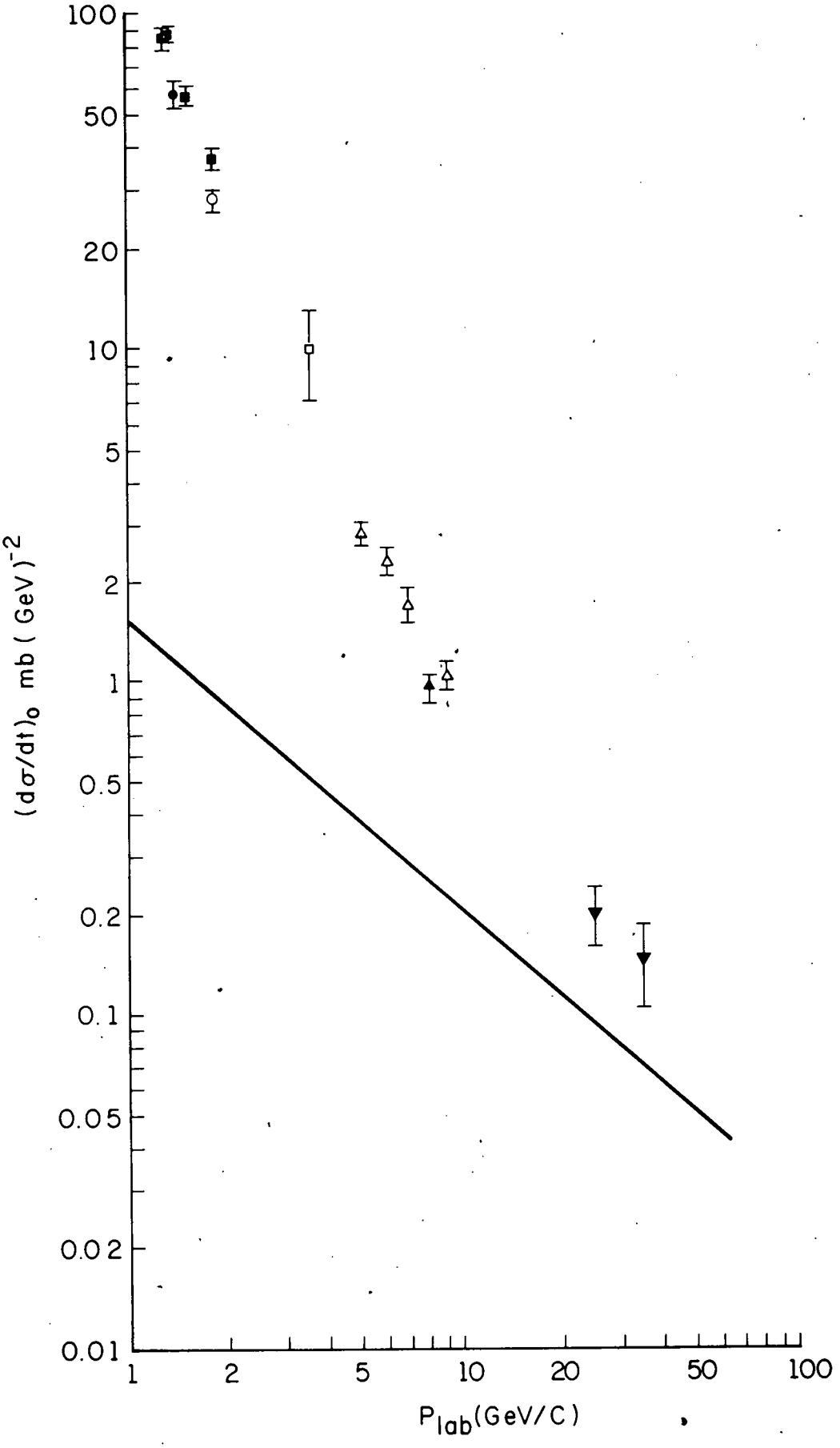
100
50
20
10
5
2
1
0.5
0.2
0.1
0.05
0.02
0.01
$(d\sigma/dt)_0$ mb (GeV)$^{-2}$
1
2
5
10
20
50
100
P_{lab}(GeV/C)

Figure 9

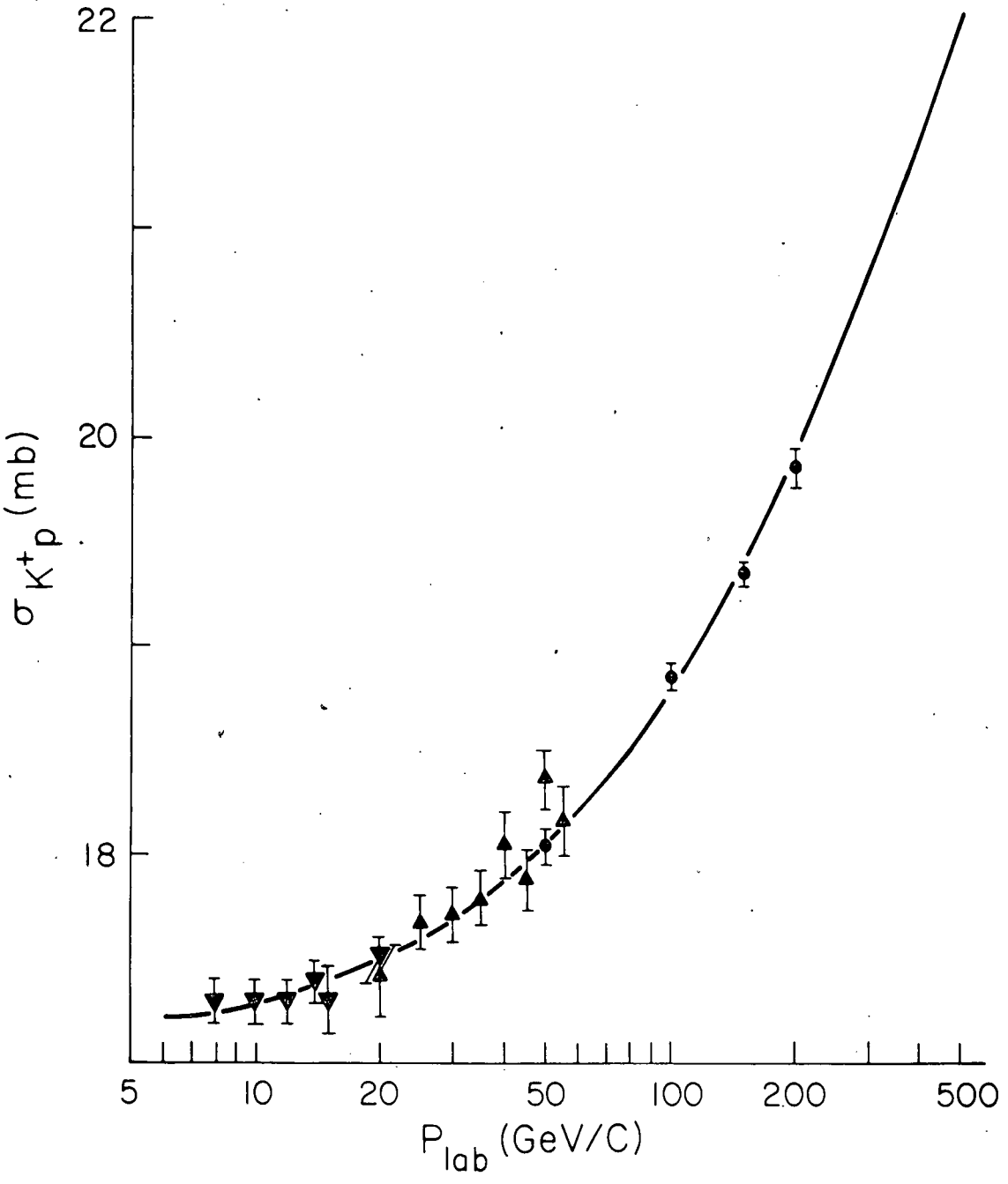

Figure 10

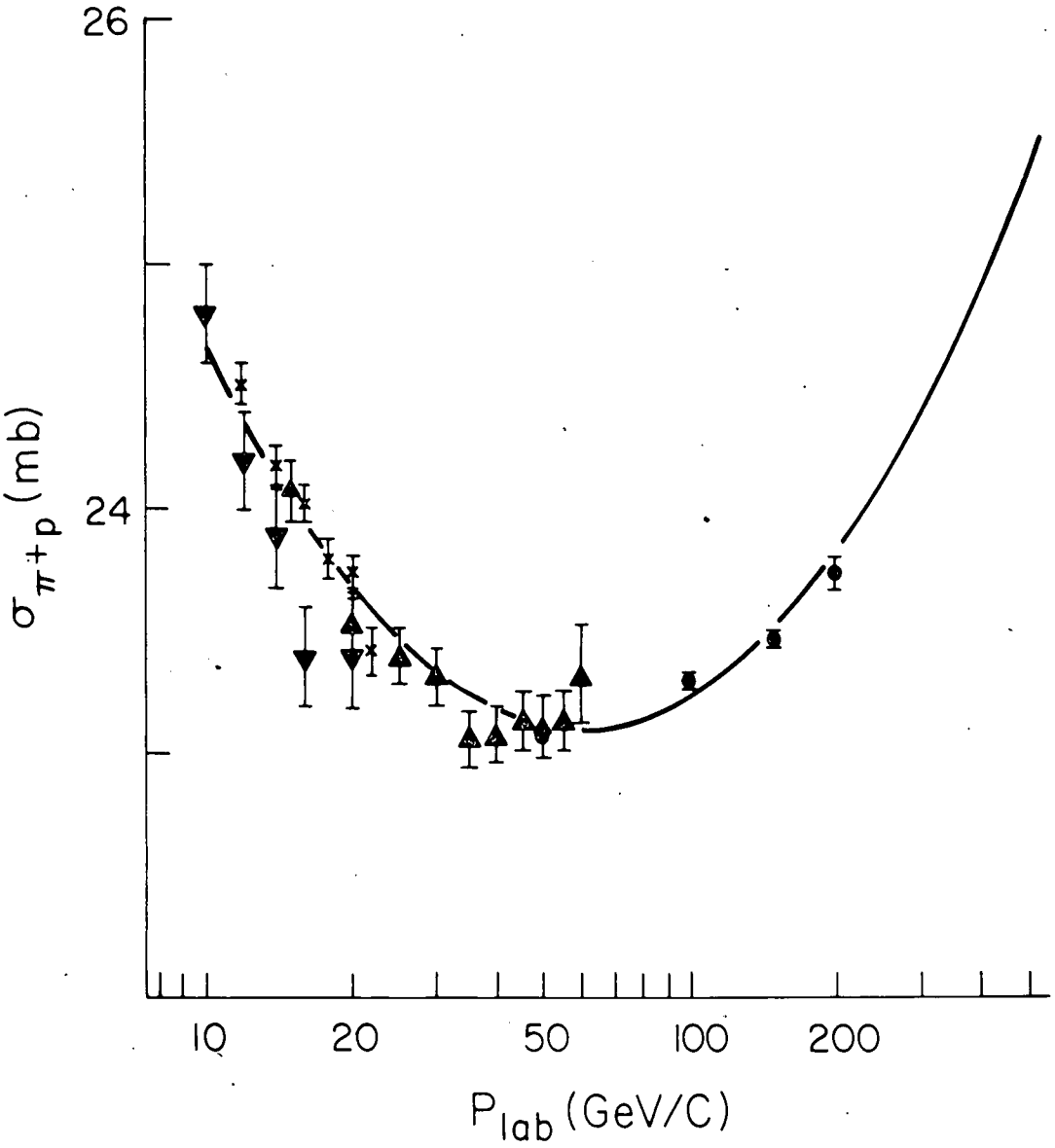

Figure 11

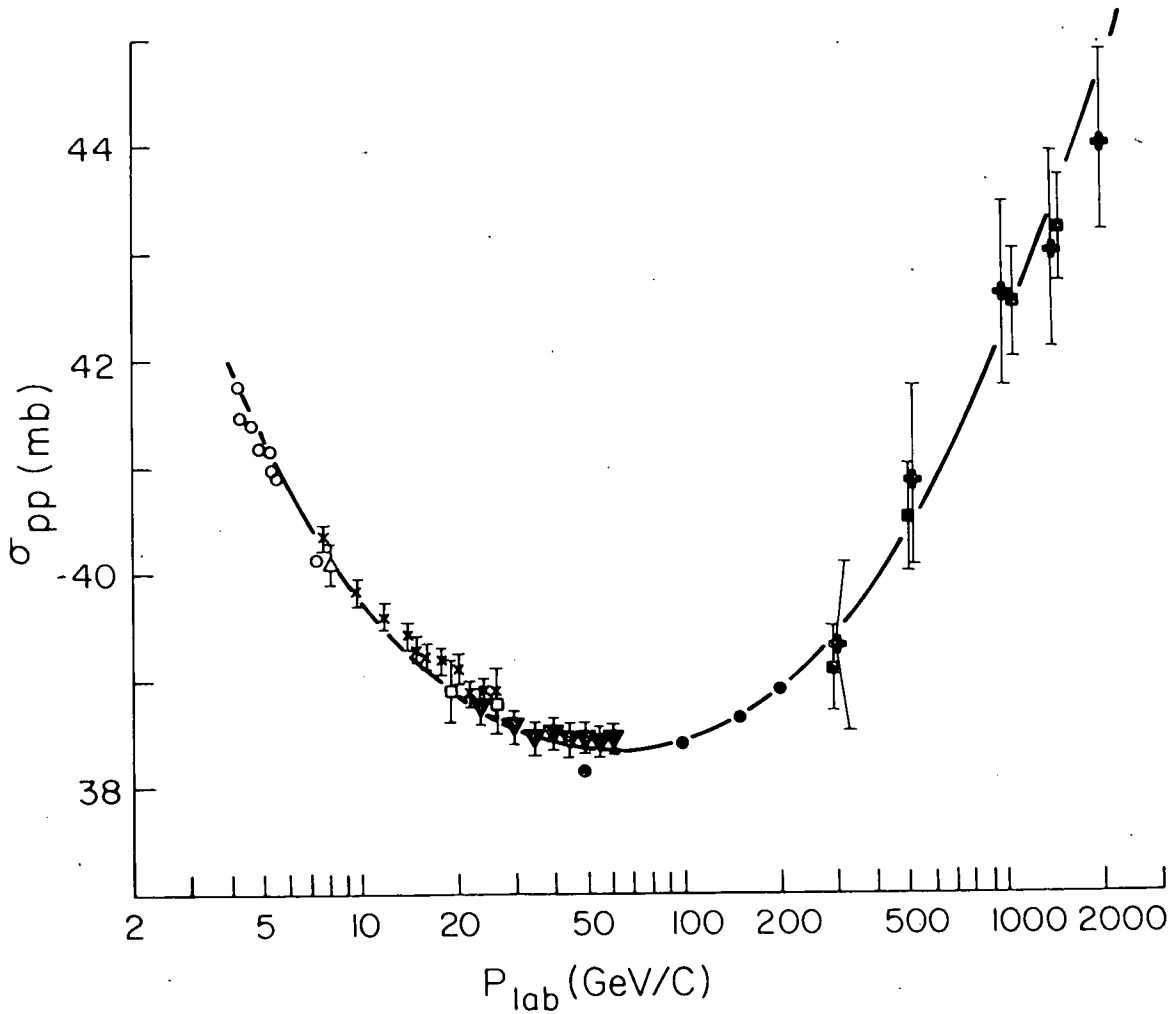
44
42
-40
38
σ_{pp} (mb)
2
5
10
20
50
100
200
500
1000
2000
P_{lab} (GeV/C)

Figure 12

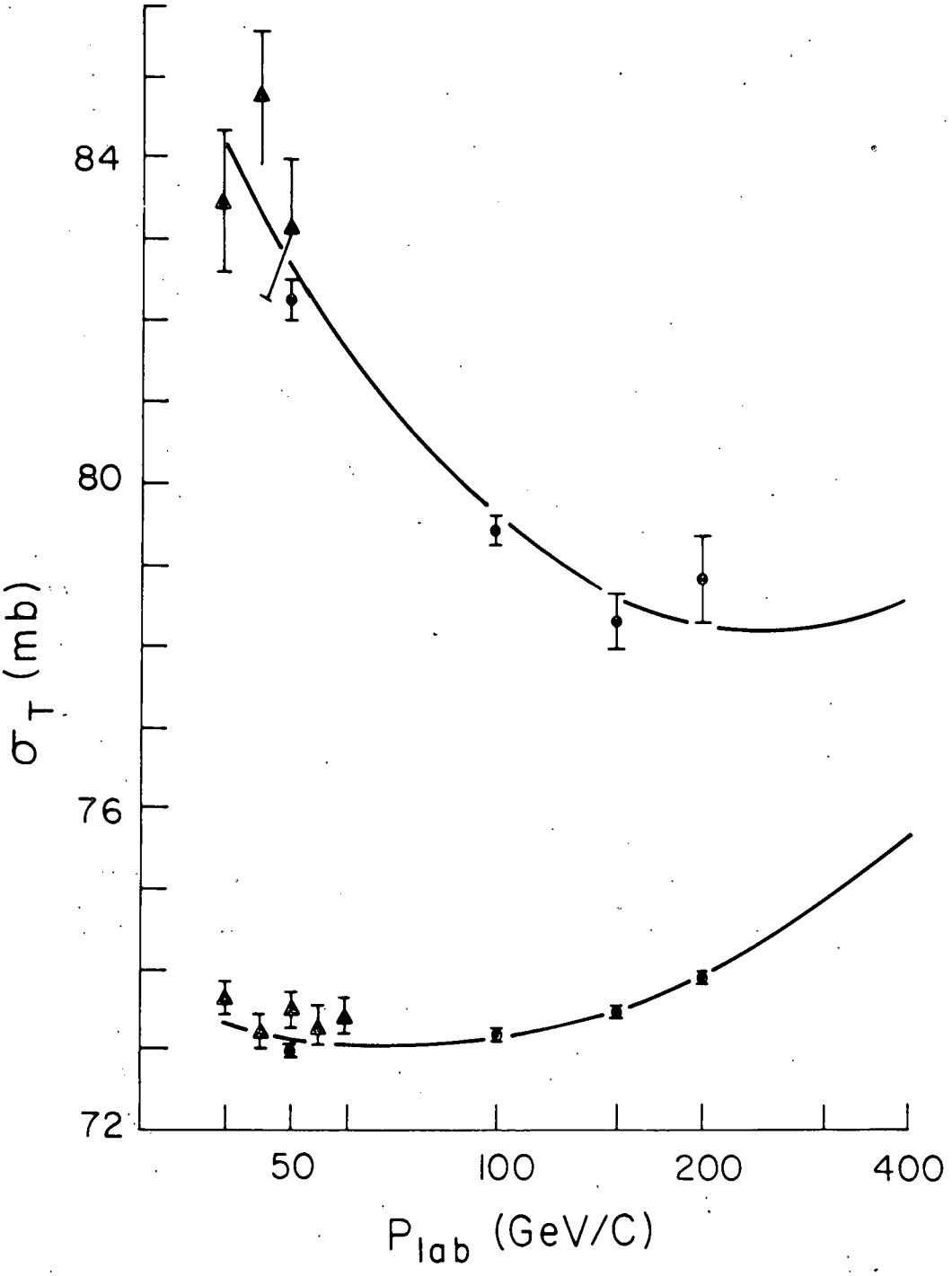

Figure 13

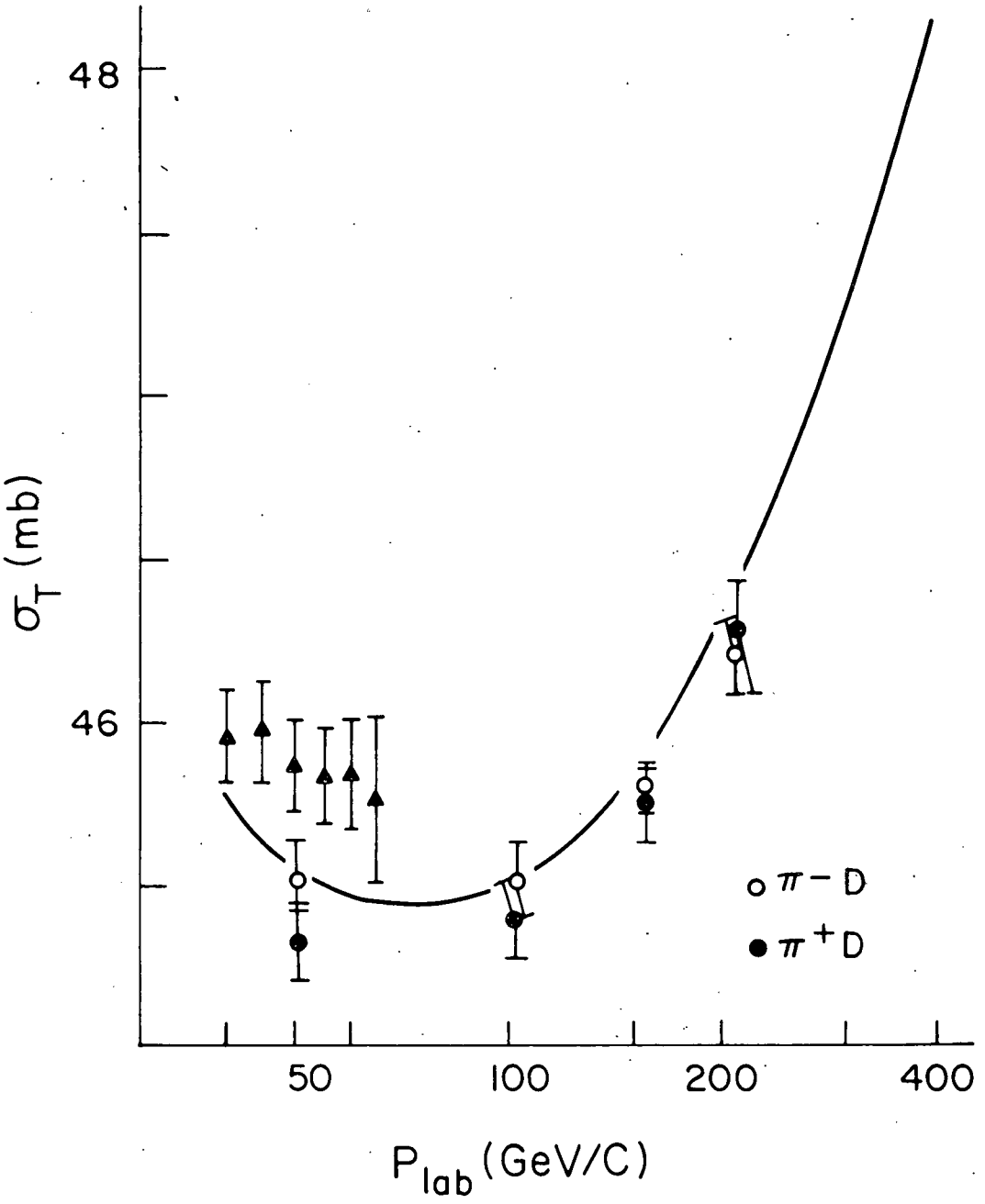

Figure 14

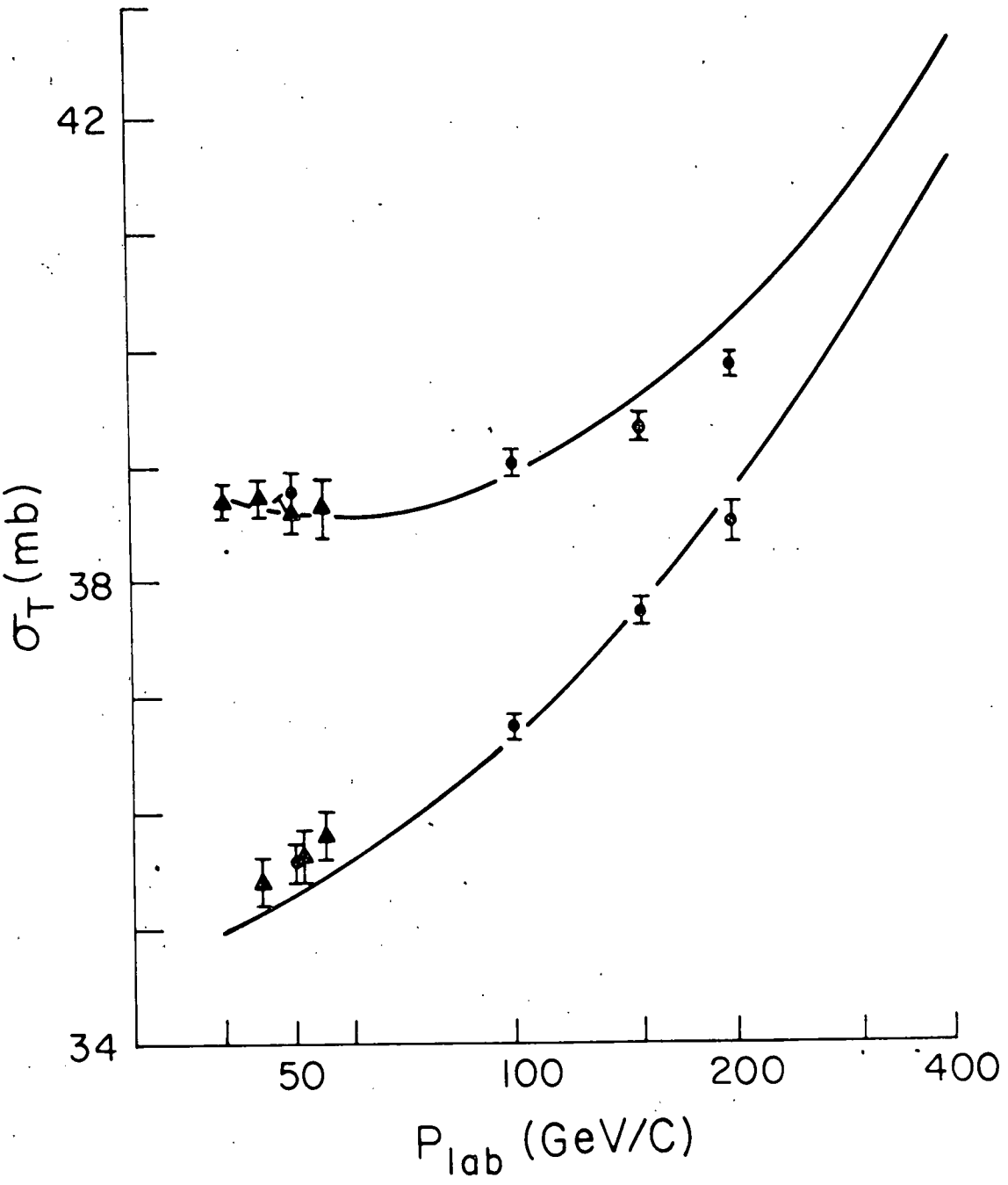

Figure 15

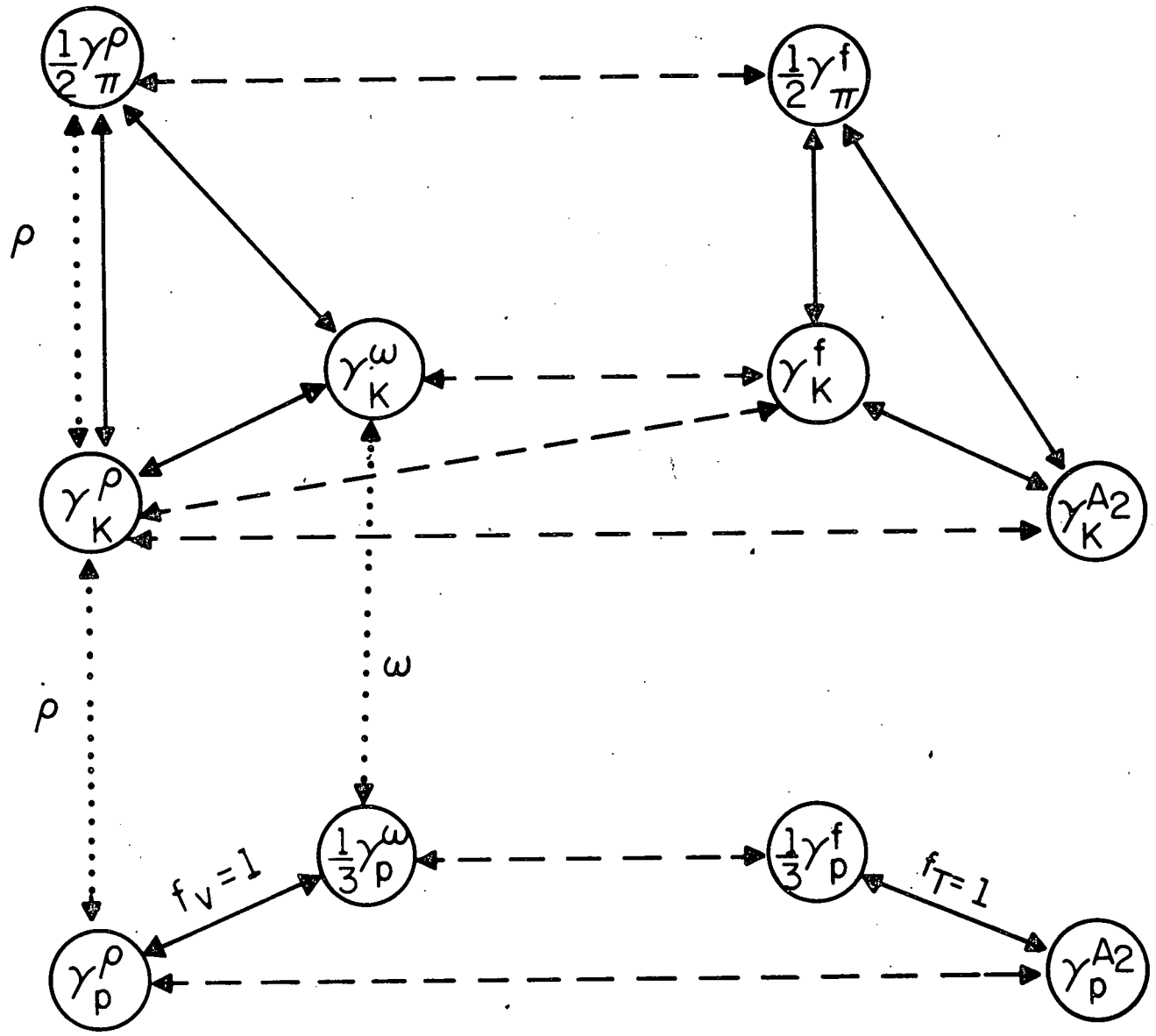
$\frac{1}{2}\gamma^{\rho}_{\pi}$
$\frac{1}{2}\gamma^{f}_{\pi}$
ρ
γ^{ω}_{K}
γ^{f}_{K}
γ^{ρ}_{K}
γ^{A2}_{K}
ω
ρ
$\frac{1}{3}\gamma^{\omega}_{p}$
$\frac{1}{3}\gamma^{f}_{p}$
$f_V = 1$
$f_T = 1$
γ^{ρ}_{p}
γ^{A2}_{p}
SU (3)
EXCHANGE DEGENERACY
UNIVERSALITY

Figure B